Multibody System Dynamics manuscript No.
(will be inserted by the editor)

Port-Hamiltonian flexible multibody dynamics

Andrea Brugnoli[1] · Daniel Alazard[1] · Valérie Pommier-Budinger[1] · Denis Matignon[1]

Received: date / Accepted: date

Abstract A new formulation for the modular construction of multibody systems is presented. By rearranging the equations for a flexible floating body and introducing the appropriate canonical momenta, the model is recast into a coupled system of ordinary and partial differential equations in port-Hamiltonian form. This approach relies on a floating frame description and stays valid under the assumption of small deformations. A finite element based method is then introduced to discretize the dynamics in a structure preserving manner. Joints are introduced by interconnecting each body to the surrounding elements in a modular way. Constraints are imposed at a velocity level, leading to an index 2 quasi linear differential-algebraic system. Numerical tests are carried out to assess the validity of the proposed approach.

Keywords Port-Hamiltonian systems · Floating frame formulation · Flexible multibody systems · Structure preserving discretization

This work is supported by the project ANR-16-CE92-0028, entitled *Interconnected Infinite-Dimensional systems for Heterogeneous Media*, INFIDHEM, financed by the French National Research Agency (ANR) and the Deutsche Forschungsgemeinschaft (DFG). Further information is available at `https://websites.isae-supaero.fr/infidhem/the-project`.

Andrea Brugnoli
E-mail: andrea.brugnoli@isae.fr

Daniel Alazard
E-mail: daniel.alazard@isae.fr

Valérie Pommier-Budinger
E-mail: valerie.budinger@isae.fr

Denis Matignon
E-mail: denis.matignon@isae.fr

[1]ISAE-SUPAERO, Université de Toulouse, France.
10 Avenue Edouard Belin, BP-54032, 31055 Toulouse Cedex 4.

1 Introduction

In structural control co-design of flexible multibody systems, it is especially useful to dispose of a modular description, to simplify analysis. In this spirit, the transfer matrix method [30] and the component mode synthesis [18] are two well known substructuring techniques that allow the construction of complex multibody systems by interconnecting subcomponents together. A reformulation of the Finite Element-Transfer Matrix (FE-TM) method [36] allows an easy construction of reduced models that are suited for decentralized control design. For the component mode synthesis, the controlled component synthesis (CCS), a framework for the design of decentralized controller of flexible structures, has been proposed in [38]. Another modeling paradigm based on the component mode synthesis is the two-input two-output port (TITOP) approach [1]. It conceives the dynamical model of each substructure as a transfer between the accelerations and the external forces at the connection points. This feature allows considering different boundary conditions by inverting specific channels in the transfer matrix. A rigorous validation was provided in [28,31], where the robustness of the methodology in handling various boundary conditions was assessed.

The Lagrangian formulation is the most commonly used methodology to retrieve the equations of motion of flexible multibody systems. However, the port-Hamiltonian (pH) framework [13] has been recently extended to describe the dynamics of rigid and flexible links [22,23]. PH systems are intrinsically modular [10], hence this approach naturally allows constructing complex system by interconnecting together atomic elements. The proposed formulation naturally accounts for the non-linearities due to large deformations. However, this methodology relies on Lie algebra and differential geometry concepts and requires non standard discretization techniques [17]. Thus, the overall implementation is not straightforward.

Together with the approach used to derive the equations of motion, the incorporation of the elastic motion represents another important point when dealing with flexible multibody systems. Three descriptions are commonly used: the floating frame formulation, the corotational frame formulation and the inertial frame formulation [15]. The choice greatly depends on the foreseen application. The corotational and inertial frame formulations allow to take into account large deformations of the elastic body, hence are well-suited for accurate simulations. Unfortunately, the application of linear model reduction techniques remains impractical [37] and the inclusion of active control strategies is unfeasible due to the computational burden. The floating frame formulation is less accurate but easily integrates many model reduction techniques [26], making it possible to obtain a low-dimensional problem for control design.

In this paper, we propose to combine the pH framework with a floating frame description of the dynamics. Starting from the general equation for the rigid flexible dynamics of a floating body, an equivalent port-Hamiltonian system is found by appropriate selection of the canonical momenta. The flexible behavior is based on the linear elasticity assumption making it possible to include models that cannot be easily formulated in terms of differential form [6,7]. The problem is then written as a coupled system of ODEs and PDEs, extending the general definition of finite-dimensional port-Hamiltonian descriptor systems provided in [24]. A suitable structure-preserving discretization method, based on [9], is then used to obtain a finite-dimensional pH system. Each individual component can then be

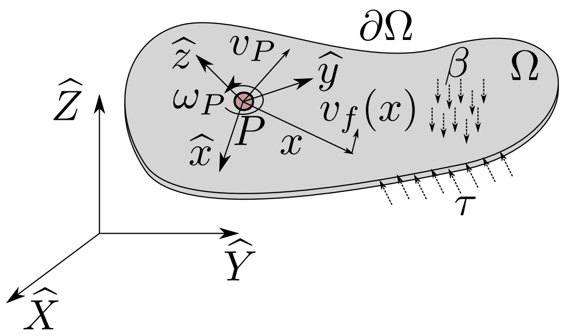

Fig. 1 Thin floating body undergoing a surface traction τ and body force density β

interconnected to the other bodies using standard interconnection of pH systems, as it is done in [23]. The constraints are imposed on the velocities and results in a quasi-linear index 2 differential-algebraic port-Hamiltonian system (pHDAE) [35, 4]. The algebraic constraints can be eliminated, preserving the overall pH structure, using null space methods [21]. The modularity feature of pH systems makes the proposed approach analogous to a substructuring technique [20]. A complex multibody system can be assembled by interconnecting blocks, allowing the usage of modeling platforms like SIMULINK® or MODELICA®. As a floating frame formulation is used, model reduction techniques can be employed to lower the computational complexity of the model [11,14]. All the features make the proposed formulation interesting for control applications, that can benefit from the properties of pH systems [25,27].

The paper is organized in the following manner. In Section 2 the classical equations of a flexible floating body, derived by means of the virtual work principle [33,34], are recalled. Using the properties of the cross product, the equations are recast in a form closer to the pH structure. Section 3 details the pH formulation of a floating flexible body by introducing the proper canonical momenta. In Section 4 a finite element based discretization is detailed for the elastodynamics problem. The procedure is then easily applied to flexible floating bodies. The particular case of thin planar beams is then detailed, as it will be then employed in the simulation part. Section 5 explains how to interconnect models together using classical pH interconnection. Section 6 is devoted to numerical examples, to assess the validity of the proposed methodology. The test cases are taken from previously published articles [12,15].

2 Flexible dynamics of a floating body

The coupled ODE-PDE system representing the motion of a single flexible body are here recalled. Then, by exploiting the properties of the cross product the system of equations is rephrased to highlight the port-Hamiltonian structure.

2.1 Classical model

Consider an open connected set $\Omega \subseteq \mathbb{R}^3$, representing a floating flexible body. The dynamics is computed at a generic point P, that is not necessarily the center of mass. The velocity of a generic point is expressed by considering a small flexible displacement superimposed to the rigid motion

$$\boldsymbol{v} = \boldsymbol{v}_P + [\boldsymbol{\omega}_P]_\times (\boldsymbol{x} + \boldsymbol{u}_f) + \boldsymbol{v}_f,$$

where $\boldsymbol{v}_P, \boldsymbol{\omega}_P$ are the linear and angular velocities of point P and $\boldsymbol{v}_f := \dot{\boldsymbol{u}}_f$ is the time derivative of the deformation displacement $\boldsymbol{u}_f$ (computed in the body frame). These quantities are evaluated in the body reference frame $\widehat{\boldsymbol{x}}, \widehat{\boldsymbol{y}}, \widehat{\boldsymbol{z}}$ (see Fig. 1). The notation $[\boldsymbol{a}]_\times$ (cross map) denotes the skew-symmetric matrix associated to vector $\boldsymbol{a}$ (see Appendix A). The model for the classical equations derived using the principle of virtual work can be found in [33] and [34, Chapter 4]. The small difference with respect to the derivation therein is that the equation for the translation is now written in the body frame (see Appendix B).

- Linear momentum balance:

$$\begin{aligned} m(\dot{\boldsymbol{v}}_P + [\boldsymbol{\omega}_P]_\times \boldsymbol{v}_P) + [\boldsymbol{s}_u]_\times^\top \dot{\boldsymbol{\omega}}_P + \int_\Omega \rho \ddot{\boldsymbol{u}}_f \, \mathrm{d}\Omega = \\ - [\boldsymbol{\omega}_P]_\times [\boldsymbol{\omega}_P]_\times \boldsymbol{s}_u - \int_\Omega 2\rho [\boldsymbol{\omega}_P]_\times \dot{\boldsymbol{u}}_f \, \mathrm{d}\Omega + \int_\Omega \boldsymbol{\beta} \, \mathrm{d}\Omega + \int_{\partial\Omega} \boldsymbol{\tau} \, \mathrm{d}\Gamma, \end{aligned} \tag{1}$$

  where ρ is the mass density, $m = \int_\Omega \rho \, \mathrm{d}\Omega$ the total mass, $\boldsymbol{s}_u = \int_\Omega \rho(\boldsymbol{x}+\boldsymbol{u}_f) \, \mathrm{d}\Omega$ the static moment. Additionally, $\boldsymbol{\beta}$ is a density force and $\boldsymbol{\tau}$ is a surface traction, both expressed in the body reference frame.
- Angular momentum balance:

$$\begin{aligned} [\boldsymbol{s}_u]_\times (\dot{\boldsymbol{v}}_P + [\boldsymbol{\omega}_P]_\times \boldsymbol{v}_P) + \boldsymbol{J}_u \dot{\boldsymbol{\omega}}_P + \int_\Omega \rho [\boldsymbol{x} + \boldsymbol{u}_f]_\times \ddot{\boldsymbol{u}}_f \, \mathrm{d}\Omega + [\boldsymbol{\omega}_P]_\times \boldsymbol{J}_u \boldsymbol{\omega}_P = \\ - \int_\Omega 2\rho [\boldsymbol{x} + \boldsymbol{u}_f]_\times [\boldsymbol{\omega}_P]_\times \dot{\boldsymbol{u}}_f \, \mathrm{d}\Omega + \int_\Omega [\boldsymbol{x} + \boldsymbol{u}_f]_\times \boldsymbol{\beta} \, \mathrm{d}\Omega + \int_{\partial\Omega} [\boldsymbol{x} + \boldsymbol{u}_f]_\times \boldsymbol{\tau} \, \mathrm{d}\Gamma, \end{aligned} \tag{2}$$

  where $\boldsymbol{J}_u := \int_\Omega \rho [\boldsymbol{x} + \boldsymbol{u}_f]_\times^\top [\boldsymbol{x} + \boldsymbol{u}_f]_\times \, \mathrm{d}\Omega = - \int_\Omega \rho [\boldsymbol{x} + \boldsymbol{u}_f]_\times [\boldsymbol{x} + \boldsymbol{u}_f]_\times \, \mathrm{d}\Omega$ is the inertia matrix.
- Flexibility PDE:

$$\begin{aligned} \rho(\dot{\boldsymbol{v}}_P + [\boldsymbol{\omega}_P]_\times \boldsymbol{v}_P) + \rho([\dot{\boldsymbol{\omega}}_P]_\times + [\boldsymbol{\omega}_P]_\times [\boldsymbol{\omega}_P]_\times)(\boldsymbol{x} + \boldsymbol{u}_f) + \rho(2[\boldsymbol{\omega}_P]_\times \dot{\boldsymbol{u}}_f + \ddot{\boldsymbol{u}}_f) = \\ \mathrm{Div}\, \boldsymbol{\Sigma} + \boldsymbol{\beta}, \end{aligned} \tag{3}$$

  Variable $\boldsymbol{\Sigma}$ is the Cauchy stress tensor. From linear elasticity theory it is well known that the infinitesimal stress is given by $\boldsymbol{\varepsilon} = \mathrm{Grad}(\boldsymbol{u}_f)$, where $\mathrm{Grad} = \frac{1}{2}[\nabla + \nabla^\top]$ is the symmetric gradient. The constitutive equation is expressed as $\boldsymbol{\Sigma} = \boldsymbol{\mathcal{D}}\boldsymbol{\varepsilon}$, where $\boldsymbol{\mathcal{D}}$ is the stiffness tensor. This PDE require the specifications of boundary conditions.

$$\begin{aligned} \boldsymbol{\Sigma} \cdot \boldsymbol{n}|_{\Gamma_N} &= \boldsymbol{\tau}|_{\Gamma_N}, \quad \boldsymbol{n} \text{ is the outward normal}, \\ \boldsymbol{u}_f|_{\Gamma_D} &= \bar{\boldsymbol{u}}_f|_{\Gamma_D}, \end{aligned} \tag{4}$$

The boundary $\partial\Omega = \Gamma_D \cup \Gamma_N$ is split into two subsets, one on which the surface traction is imposed (Γ_N Neumann condition) and the other where the flexible displacement is known (Γ_D Dirichlet condition).

2.2 Towards a pH formulation

The gyroscopic term in Eqs. (1), (2), (3) need some manipulation so that the skew-symmetric interconnection operator can be more easily highlighted. Considering that $\dot{\boldsymbol{v}}_f = \ddot{\boldsymbol{u}}_f$ and using the Jacobi identity (51) (see Appendix B for a detailed explanation) the classical equations can be equivalently rewritten as follows.

– Linear momentum balance:

$$\begin{gathered} m\dot{\boldsymbol{v}}_P + [\boldsymbol{s}_u]_\times^\top \dot{\boldsymbol{\omega}}_P + \int_\Omega \rho \dot{\boldsymbol{v}}_f \, \mathrm{d}\Omega = \\ \left[m\boldsymbol{v}_P + [\boldsymbol{s}_u]_\times^\top \boldsymbol{\omega}_P + 2\int_\Omega \rho \boldsymbol{v}_f \, \mathrm{d}\Omega \right]_\times \boldsymbol{\omega}_P + \int_\Omega \boldsymbol{\beta} \, \mathrm{d}\Omega + \int_{\partial\Omega} \boldsymbol{\tau} \, \mathrm{d}\Gamma. \end{gathered} \tag{5}$$

– Angular momentum balance:

$$\begin{gathered} [\boldsymbol{s}_u]_\times \dot{\boldsymbol{v}}_P + \boldsymbol{J}_u \dot{\boldsymbol{\omega}}_P + \int_\Omega \rho [\boldsymbol{x} + \boldsymbol{u}_f]_\times \dot{\boldsymbol{v}}_f \, \mathrm{d}\Omega = \\ \left[[\boldsymbol{s}_u]_\times^\top \boldsymbol{\omega}_P + 2\int_\Omega \rho \boldsymbol{v}_f \, \mathrm{d}\Omega \right]_\times \boldsymbol{v}_P + \left[[\boldsymbol{s}_u]_\times \boldsymbol{v}_P + \boldsymbol{J}_u \boldsymbol{\omega}_P + 2\int_\Omega \rho [\boldsymbol{x} + \boldsymbol{u}_f]_\times \boldsymbol{v}_f \, \mathrm{d}\Omega \right]_\times \boldsymbol{\omega}_P + \\ 2\int_\Omega \left[\rho \boldsymbol{v}_P + \rho [\boldsymbol{x} + \boldsymbol{u}_f]_\times^\top \boldsymbol{\omega}_P \right]_\times \boldsymbol{v}_f \, \mathrm{d}\Omega + \int_\Omega [\boldsymbol{x} + \boldsymbol{u}_f]_\times \boldsymbol{\beta} \, \mathrm{d}\Omega + \int_{\partial\Omega} [\boldsymbol{x} + \boldsymbol{u}_f]_\times \boldsymbol{\tau} \, \mathrm{d}\Gamma. \end{gathered} \tag{6}$$

– Flexibility PDE:

$$\begin{gathered} \rho \dot{\boldsymbol{v}}_P + \rho [\boldsymbol{x} + \boldsymbol{u}_f]_\times^\top \dot{\boldsymbol{\omega}}_P + \rho \dot{\boldsymbol{v}}_f = \\ \left[\rho \boldsymbol{v}_P + \rho [\boldsymbol{x} + \boldsymbol{u}_f]_\times^\top \boldsymbol{\omega}_P + 2\rho \boldsymbol{v}_f \right]_\times \boldsymbol{\omega}_P + \mathrm{Div}\, \boldsymbol{\Sigma} + \boldsymbol{\beta}. \end{gathered} \tag{7}$$

Again this equation requires the specification of the boundary conditions (4).

Introduction the appropriate momenta, this model can be reformulated as a pH system as illustrated in the following section.

3 Elastic body under large rigid motion as a pH system

In this section the flexible dynamics of a floating body is written as a coupled system of ODEs and PDEs in pH form. The final form is a descriptor port-Hamiltonian system that fits and generalizes the framework detailed in [4,24].

3.1 Energies and canonical momenta

Consider the total energy (Hamiltonian), given by the sum of kinetic and deformation energy:

$$
\begin{aligned}
H &= H_{\text{kin}} + H_{\text{def}}, \\
&= \frac{1}{2}\int_{\Omega} \left\{ \rho ||\boldsymbol{v}_P + [\boldsymbol{\omega}_P]_\times (\boldsymbol{x} + \boldsymbol{u}_f) + \boldsymbol{v}_f||^2 + \boldsymbol{\Sigma} : \boldsymbol{\varepsilon} \right\} \, \mathrm{d}\Omega.
\end{aligned} \tag{8}
$$

The inner product $\boldsymbol{A}:\boldsymbol{B} = \mathrm{Tr}(\boldsymbol{A}\boldsymbol{B}^T)$ is the tensor contraction. The momenta (usually called energy variables in the pH framework) are then computed by derivation of the Hamiltonian. As the variables belong to finite- and infinite-dimensional spaces the derivative is either a classical gradient or a variational derivative:

$$
\begin{aligned}
\boldsymbol{p}_t &:= \frac{\partial H}{\partial \boldsymbol{v}_P} = m\boldsymbol{v}_P + [\boldsymbol{s}_u]_\times^\top \boldsymbol{\omega}_P + \int_\Omega \rho \boldsymbol{v}_f \, \mathrm{d}\Omega, \\
\boldsymbol{p}_r &:= \frac{\partial H}{\partial \boldsymbol{\omega}_P} = [\boldsymbol{s}_u]_\times \boldsymbol{v}_P + \boldsymbol{J}_u \boldsymbol{\omega}_P + \int_\Omega \rho [\boldsymbol{x} + \boldsymbol{u}_f]_\times \boldsymbol{v}_f \, \mathrm{d}\Omega, \\
\boldsymbol{p}_f &:= \frac{\delta H}{\delta \boldsymbol{v}_f} = \rho \boldsymbol{v}_P + \rho[\boldsymbol{x} + \boldsymbol{u}_f]_\times^\top \boldsymbol{\omega}_P + \rho \boldsymbol{v}_f, \\
\boldsymbol{\varepsilon} &:= \frac{\delta H}{\delta \boldsymbol{\Sigma}} = \boldsymbol{\mathcal{D}}^{-1} \boldsymbol{\Sigma},
\end{aligned} \tag{9}
$$

where the last derivative is computed with respect to a tensor [6]. The relation between energy and co-energy variable is then given by

$$
\begin{bmatrix} \boldsymbol{p}_t \\ \boldsymbol{p}_r \\ \boldsymbol{p}_f \\ \boldsymbol{\varepsilon} \end{bmatrix} = \underbrace{\begin{bmatrix} m\boldsymbol{I}_{3\times 3} & [\boldsymbol{s}_u]_\times^\top & \mathcal{I}_\rho^\Omega & 0 \\ [\boldsymbol{s}_u]_\times & \boldsymbol{J}_u & \boldsymbol{\mathcal{I}}_{\rho x}^\Omega & 0 \\ (\mathcal{I}_\rho^\Omega)^* & (\boldsymbol{\mathcal{I}}_{\rho x}^\Omega)^* & \rho & 0 \\ 0 & 0 & 0 & \boldsymbol{\mathcal{D}}^{-1} \end{bmatrix}}_{\boldsymbol{\mathcal{M}}:\ \text{Mass operator}} \begin{bmatrix} \boldsymbol{v}_P \\ \boldsymbol{\omega}_P \\ \boldsymbol{v}_f \\ \boldsymbol{\Sigma} \end{bmatrix}, \tag{10}
$$

where $\boldsymbol{I}_{3\times 3}$ is the identity matrix in $\mathbb{R}^3$. and the operators are defined as

$$
\begin{aligned}
\mathcal{I}_\rho^\Omega &:= \int_\Omega \rho(\cdot) \, \mathrm{d}\Omega, & \boldsymbol{\mathcal{I}}_{\rho x}^\Omega &:= \int_\Omega \rho[\boldsymbol{x} + \boldsymbol{u}_f]_\times (\cdot) \, \mathrm{d}\Omega, \\
(\mathcal{I}_\rho^\Omega)^* &= \rho, & (\boldsymbol{\mathcal{I}}_{\rho x}^\Omega)^* &= \rho[\boldsymbol{x} + \boldsymbol{u}_f]_\times^\top = -\rho[\boldsymbol{x} + \boldsymbol{u}_f]_\times.
\end{aligned}
$$

The superscript $*$ denotes the adjoint operator. The mass operator $\boldsymbol{\mathcal{M}}$ is a self-adjoint, positive operator. The kinetic and deformation energy can then be written as

$$
H_{\text{kin}} + H_{\text{def}} = \frac{1}{2}\langle \boldsymbol{e}_{\text{kd}}, \ \boldsymbol{\mathcal{M}} \boldsymbol{e}_{\text{kd}} \rangle \tag{11}
$$

where $\boldsymbol{e}_{\text{kd}} = [\boldsymbol{v}_P; \, \boldsymbol{\omega}_P; \, \boldsymbol{v}_f; \boldsymbol{\Sigma}]$ and the inner product $\langle \ , \ \rangle$ is taken over the space $\mathbb{R}^3 \times \mathbb{R}^3 \times \mathscr{L}^2(\Omega, \mathbb{R}^3) \times \mathscr{L}^2(\Omega, \mathbb{R}^{3\times 3})$ ($\mathscr{L}^2$ is the space of square integrable functions). Notice that the kinetic energy also depends on the flexible displacement:

$$
\frac{\delta H_{\text{kin}}}{\delta \boldsymbol{u}_f} = [\boldsymbol{p}_f]_\times \boldsymbol{\omega}_{\boldsymbol{P}}
$$

This term is responsible for a coupling between the kinematic coordinates and the velocities, as it will be clear in the following section.

3.2 PH formulation

In order to get a complete formulation generalized coordinates are required. It is natural to select the following variables:

- ${}^i\boldsymbol{r}_P$: the position of point P in the inertial frame of reference;
- $\boldsymbol{R}$: the direction cosine matrix that transforms vectors from the body frame to the inertial frame (other attitude parametrization are possible, here the orientation matrix is considered for ease of presentation);
- $\boldsymbol{u}_f$ the flexible displacement;

In particular, following [16], the direction cosine matrix matrix is converted in a vector by concatenating its rows

$$\boldsymbol{R}_{\mathrm{v}} = \mathrm{vec}(\boldsymbol{R}^\top) = [\boldsymbol{R}_x \ \boldsymbol{R}_y \ \boldsymbol{R}_z]^\top,$$

where $\boldsymbol{R}_x, \boldsymbol{R}_y, \boldsymbol{R}_z$ are the first, second and third row of matrix $\boldsymbol{R}$. Furthermore the corresponding cross map will be given by

$$[\boldsymbol{R}_{\mathrm{v}}]_\times = \begin{bmatrix} [\boldsymbol{R}_x]_\times \\ [\boldsymbol{R}_y]_\times \\ [\boldsymbol{R}_z]_\times \end{bmatrix}, \qquad [\boldsymbol{R}_{\mathrm{v}}]_\times : \mathbb{R}^9 \to \mathbb{R}^{9\times 3}.$$

The overall port-Hamiltonian formulation, equivalent to Eqs. (5), (6), (7), is then (omitting the external forces and torques)

$$\underbrace{\begin{bmatrix} \boldsymbol{I} & 0 \\ 0 & \boldsymbol{\mathcal{M}} \end{bmatrix}}_{\boldsymbol{\mathcal{E}}} \frac{d}{dt} \underbrace{\begin{bmatrix} {}^i\mathbf{r}_P \\ \boldsymbol{R}_{\mathrm{v}} \\ \boldsymbol{u}_f \\ \boldsymbol{v}_P \\ \boldsymbol{\omega}_P \\ \boldsymbol{v}_f \\ \boldsymbol{\Sigma} \end{bmatrix}}_{\boldsymbol{e}} = \underbrace{\left[\begin{array}{ccc|cccc} 0 & 0 & 0 & \boldsymbol{R} & 0 & 0 & 0 \\ 0 & 0 & 0 & 0 & [\boldsymbol{R}_{\mathrm{v}}]_\times & 0 & 0 \\ 0 & 0 & 0 & 0 & 0 & \boldsymbol{I}_{3\times 3} & 0 \\ \hline -\boldsymbol{R}^\top & 0 & 0 & 0 & [\widetilde{\boldsymbol{p}}_t]_\times & 0 & 0 \\ 0 & -[\boldsymbol{R}_{\mathrm{v}}]_\times^\top & 0 & [\widetilde{\boldsymbol{p}}_t]_\times & [\widetilde{\boldsymbol{p}}_r]_\times & \boldsymbol{\mathcal{I}}_{p_f}^{\Omega} & 0 \\ 0 & 0 & -\boldsymbol{I}_{3\times 3} & 0 & -(\boldsymbol{\mathcal{I}}_{p_f}^{\Omega})^* & 0 & \mathrm{Div} \\ 0 & 0 & 0 & 0 & 0 & \mathrm{Grad} & 0 \end{array}\right]}_{\boldsymbol{\mathcal{J}}} \underbrace{\begin{bmatrix} \partial_{\boldsymbol{r}_P} H \\ \partial_{\boldsymbol{R}_{\mathrm{v}}} H \\ \delta_{\boldsymbol{u}_f} H \\ \boldsymbol{v}_P \\ \boldsymbol{\omega}_P \\ \boldsymbol{v}_f \\ \boldsymbol{\Sigma} \end{bmatrix}}_{\boldsymbol{z}}. \tag{12}$$

Variables $\widetilde{\boldsymbol{p}}_t, \widetilde{\boldsymbol{p}}_r$ are defined as

$$\begin{aligned} \widetilde{\boldsymbol{p}}_t &= \boldsymbol{p}_t + \int_\Omega \rho \boldsymbol{v}_f \, \mathrm{d}\Omega, \\ \widetilde{\boldsymbol{p}}_r &= \boldsymbol{p}_r + \int_\Omega \rho [\boldsymbol{x} + \boldsymbol{u}_f]_\times \boldsymbol{v}_f \, \mathrm{d}\Omega. \end{aligned} \tag{13}$$

The operator $\boldsymbol{\mathcal{I}}_{p_f}^{\Omega}$ is defined as

$$\boldsymbol{\mathcal{I}}_{p_f}^{\Omega} := \int_\Omega \left\{ 2[\boldsymbol{p}_f]_\times + \rho[\boldsymbol{v}_f]_\times \right\} (\cdot) \, \mathrm{d}\Omega. \tag{14}$$

Its formal adjoint is given by

$$(\boldsymbol{\mathcal{I}}_{p_f}^{\Omega})^* = \left\{ 2[\boldsymbol{p}_f]_\times^\top + \rho[\boldsymbol{v}_f]_\times^\top \right\} (\cdot) = -\left\{ 2[\boldsymbol{p}_f]_\times + \rho[\boldsymbol{v}_f]_\times \right\} (\cdot)$$

The 2 coefficient is required to compensate the contribution given by $\delta_{\boldsymbol{u}_f} H$

$$-\frac{\delta H}{\delta \boldsymbol{u}_f} - (\boldsymbol{\mathcal{I}}_{p_f}^{\Omega})^* \boldsymbol{\omega}_P = \left[\rho \boldsymbol{v}_P + \rho [\boldsymbol{x} + \boldsymbol{u}_f]_\times^\top \boldsymbol{\omega}_P + 2\rho \boldsymbol{v}_f\right]_\times \boldsymbol{\omega}_P.$$

The additional terms related to $\rho \boldsymbol{v}_f$ are associated to the Coriolis accelerations that affect the deformation field. It is important to underline that Div and Grad are formally skew-adjoint operators, i.e. for homogeneous boundary conditions (I.B.P. stays for integration by parts)

$$\begin{aligned}
\int_\Omega \boldsymbol{\Sigma} : \mathrm{Grad}(\boldsymbol{v}_f) \, \mathrm{d}\Omega \underbrace{=}_{\text{I.B.P.}} -\int_\Omega \mathrm{Div}(\boldsymbol{\Sigma}) \cdot \boldsymbol{v}_f \, \mathrm{d}\Omega, \\
\langle \boldsymbol{\Sigma}, \, \mathrm{Grad}(\boldsymbol{v}_f) \rangle_{\mathscr{L}^2(\Omega, \mathbb{R}^{3\times 3}_{\text{sym}})} \underbrace{=}_{\text{I.B.P.}} - \langle \mathrm{Div}(\boldsymbol{\Sigma}), \, \boldsymbol{v}_f \rangle_{\mathscr{L}^2(\Omega, \mathbb{R}^3)},
\end{aligned}$$

where $\langle , \rangle_{\mathscr{H}}$ denote an inner product over the Hilbert space $\mathscr{H}$.
$\mathscr{L}^2(\Omega, \mathbb{R}^3)$, $\mathscr{L}^2(\Omega, \mathbb{R}^{3\times 3}_{\text{sym}})$ are the spaces of square integrable vector-valued or symmetric tensors-valued functions in $\mathbb{R}^3$. For this reason the operator $\boldsymbol{\mathcal{J}}$ is skew-symmetric $\boldsymbol{\mathcal{J}}^* = -\boldsymbol{\mathcal{J}}$.

System (12) fits into the framework detailed in [24] and extends it since a coupled system of ODEs and PDEs is considered. The state space for system (12) is

$$\mathscr{X} = \mathbb{R}^3 \times \mathbb{R}^9 \times \mathscr{L}^2(\Omega, \mathbb{R}^3) \times \mathbb{R}^3 \times \mathbb{R}^3 \times \mathscr{L}^2(\Omega, \mathbb{R}^3) \times \mathscr{L}^2(\Omega, \mathbb{R}^{3\times 3}_{\text{sym}}).$$

The dynamics can be rewritten compactly as follows

$$\begin{aligned}
\boldsymbol{\mathcal{E}}(\boldsymbol{e}) \frac{\partial \boldsymbol{e}}{\partial t} &= \boldsymbol{\mathcal{J}}(\boldsymbol{e}) \boldsymbol{z}(\boldsymbol{e}) + \boldsymbol{\mathcal{B}}_d(\boldsymbol{e}) \boldsymbol{u}_d + \boldsymbol{\mathcal{B}}_r(\boldsymbol{e}) \boldsymbol{u}_\partial, \\
\boldsymbol{y}_d &= \boldsymbol{\mathcal{B}}_d^*(\boldsymbol{e}) \boldsymbol{z}(\boldsymbol{e}), \\
\boldsymbol{y}_r &= \boldsymbol{\mathcal{B}}_r^*(\boldsymbol{e}) \boldsymbol{z}(\boldsymbol{e}), \\
\boldsymbol{u}_\partial &= \boldsymbol{\mathcal{B}}_\partial \boldsymbol{z}(\boldsymbol{e}) = \boldsymbol{\Sigma} \cdot \boldsymbol{n}|_{\partial\Omega}, \\
\boldsymbol{y}_\partial &= \boldsymbol{\mathcal{C}}_\partial \boldsymbol{z}(\boldsymbol{e}) = \boldsymbol{v}_f|_{\partial\Omega},
\end{aligned} \tag{15}$$

where $\boldsymbol{u}_d = \boldsymbol{\beta}$. Using definitions (9), it follows that the Hamiltonian satisfies

$$\partial_{\boldsymbol{e}} H = \boldsymbol{\mathcal{E}}^* \boldsymbol{z}. \tag{16}$$

Adopting the same nomenclature as in [24], $\boldsymbol{e}$ contains the state and $\boldsymbol{z}$ contains the effort functions. The operators verify $\boldsymbol{\mathcal{E}} = \boldsymbol{\mathcal{E}}^*$, $\boldsymbol{\mathcal{J}} = -\boldsymbol{\mathcal{J}}^*$. The control operators are expressed as

$$\begin{aligned}
\boldsymbol{\mathcal{B}}_d &= \left[0 \; 0 \; 0 \; \mathcal{I}^\Omega \; \boldsymbol{\mathcal{I}}_x^\Omega \; \boldsymbol{I} \; 0\right]^\top, \\
\boldsymbol{\mathcal{B}}_r &= \left[0 \; 0 \; 0 \; \mathcal{I}^\Gamma \; \boldsymbol{\mathcal{I}}_x^\Gamma \; 0 \; 0\right]^\top,
\end{aligned}$$

where

$$\begin{aligned}
\mathcal{I}^\Omega &:= \int_\Omega (\cdot) \, \mathrm{d}\Omega, & \boldsymbol{\mathcal{I}}_x^\Omega &:= \int_\Omega [\boldsymbol{x} + \boldsymbol{u}_f]_\times (\cdot) \, \mathrm{d}\Omega, \\
\mathcal{I}^\Gamma &:= \int_{\partial\Omega} (\cdot) \, \mathrm{d}\Gamma, & \boldsymbol{\mathcal{I}}_x^\Gamma &:= \int_{\partial\Omega} [\boldsymbol{x} + \boldsymbol{u}_f]_\times (\cdot) \, \mathrm{d}\Gamma.
\end{aligned}$$

The distributed control operator $\boldsymbol{\mathcal{B}}_d$ is compact. The boundary traction force acts on the rigid part through the compact operator $\boldsymbol{\mathcal{B}}_r$. Notice that by definition of adjoint (see Appendix A) vector $\boldsymbol{y}_r$ represents the rigid body displacement at the boundary

$$\boldsymbol{y}_r = (\boldsymbol{v}_P + [\boldsymbol{x} + \boldsymbol{u}_f]_\times^\top \boldsymbol{\omega}_P)|_{\partial\Omega}.$$

The power balance is naturally embedded in the dynamics

$$\begin{aligned}
\dot{H}(\boldsymbol{e}) &= \langle \partial_{\boldsymbol{e}} H, \partial_t \boldsymbol{e} \rangle_{\mathscr{X}} = \langle \boldsymbol{\mathcal{E}}^* \boldsymbol{z}, \partial_t \boldsymbol{e} \rangle_{\mathscr{X}}, \\
&= \langle \boldsymbol{z}, \boldsymbol{\mathcal{E}} \partial_t \boldsymbol{e} \rangle_{\mathscr{X}}, \quad \text{Self-adjointness of } \boldsymbol{\mathcal{E}}, \\
&= \langle \boldsymbol{z}, \boldsymbol{\mathcal{J}} \boldsymbol{z} + \boldsymbol{\mathcal{B}}_d(\boldsymbol{e}) \boldsymbol{u}_d + \boldsymbol{\mathcal{B}}_r(\boldsymbol{e}) \boldsymbol{u}_\partial \rangle_{\mathscr{X}}, \\
&= \langle \boldsymbol{y}_\partial, \boldsymbol{u}_\partial \rangle_{\mathscr{L}^2(\partial\Omega, \mathbb{R}^3)} + \langle \boldsymbol{\mathcal{B}}_d^* \boldsymbol{z}, \boldsymbol{u}_d \rangle_{\mathscr{X}} + \langle \boldsymbol{\mathcal{B}}_r^* \boldsymbol{z}, \boldsymbol{u}_\partial \rangle_{\mathscr{X}}, \quad \text{I.B.P. on } \boldsymbol{\mathcal{J}}, \\
&= \langle \boldsymbol{y}_\partial + \boldsymbol{y}_r, \boldsymbol{u}_\partial \rangle_{\mathscr{L}^2(\partial\Omega, \mathbb{R}^3)} + \langle \boldsymbol{y}_d, \boldsymbol{u}_d \rangle_{\mathscr{L}^2(\Omega, \mathbb{R}^3)},
\end{aligned} \tag{17}$$

where the integration by parts (Stokes theorem) has been used

$$\int_\Omega \boldsymbol{\Sigma} : \mathrm{Grad}(\boldsymbol{v}_f) \, \mathrm{d}\Omega + \int_\Omega \mathrm{Div}(\boldsymbol{\Sigma}) \cdot \boldsymbol{v}_f \, \mathrm{d}\Omega = \int_{\partial\Omega} (\boldsymbol{\Sigma} \cdot \boldsymbol{n}) \cdot \boldsymbol{v}_f \, \mathrm{d}\Gamma = \langle \boldsymbol{y}_\partial, \boldsymbol{u}_\partial \rangle_{\mathscr{L}^2(\partial\Omega)}. \tag{18}$$

The power balance equals the power due to body force and surface traction

$$\dot{H}(\boldsymbol{e}) = \int_{\partial\Omega} (\boldsymbol{\Sigma} \cdot \boldsymbol{n}) \cdot \boldsymbol{v} \, \mathrm{d}\Gamma + \int_\Omega \boldsymbol{u}_d \cdot \boldsymbol{v} \, \mathrm{d}\Omega, \quad \boldsymbol{v} := \boldsymbol{v}_P + [\boldsymbol{\omega}_P]_\times (\boldsymbol{x} + \boldsymbol{u}_f) + \boldsymbol{v}_f. \tag{19}$$

Even if three dimensional elasticity has been taken as example up to this point, other models are easily considered. Beam and plate models [6, 7] are described by appropriate differential operators that replace the Div, Grad appearing in (12) (see §4.3).

Remark 1 Conservative forces are easily accounted for by introducing an appropriate potential energy. For example if the gravity force is considered, the corresponding potential reads

$$H_{\mathrm{pot}} = \int_\Omega \rho g \, {}^i r_z \, \mathrm{d}\Omega = \int_\Omega \rho g \left[{}^i r_{P,z} + \boldsymbol{R}_z (\boldsymbol{x} + \boldsymbol{u}_f) \right] \, \mathrm{d}\Omega,$$

where ${}^i r_z$ is the vertical location of a generic point computed in the inertial frame. The associated co-energy variables are easily obtained

$$\begin{aligned}
\partial_{\boldsymbol{r}_P} H_{\mathrm{pot}} &= mg \, \widehat{\boldsymbol{Z}}, \quad \widehat{\boldsymbol{Z}} \text{ is the inertial frame vertical direction}, \\
\partial_{\boldsymbol{R}_{\mathrm{v}}} H_{\mathrm{pot}} &= [\boldsymbol{0}_{(3,1)}, \, \boldsymbol{0}_{(3,1)}, \, \int_\Omega \rho g (\boldsymbol{x} + \boldsymbol{u}_f)^\top \, \mathrm{d}\Omega]^\top, \\
\delta_{\boldsymbol{u}_f} H_{\mathrm{pot}} &= \rho g \, \boldsymbol{R}_z^\top.
\end{aligned}$$

These correspond to the forcing terms due to gravity.

Remark 2 The linear elasticity hypothesis does not allow to include the effect of non linearities due to large deformations. However, geometric stiffening could be considered by adding a potential energy associated to centrifugal forces [33].

Remark 3 If case of vanishing deformations $\boldsymbol{u}_f \equiv 0$ the Newton-Euler equations on the Euclidean group $SE(3)$ are retrieved

$$\begin{bmatrix} {}^{i}\dot{\boldsymbol{r}}_P \\ \boldsymbol{R}_\mathrm{v} \\ \dot{\boldsymbol{p}}_t \\ \dot{\boldsymbol{p}}_r \end{bmatrix} = \begin{bmatrix} 0 & 0 & \boldsymbol{R} & 0 \\ 0 & 0 & 0 & [\boldsymbol{R}_\mathrm{v}]_\times \\ -\boldsymbol{R}^\top & 0 & 0 & [\boldsymbol{p}_t]_\times \\ 0 & -[\boldsymbol{R}_\mathrm{v}]_\times^\top & [\boldsymbol{p}_t]_\times & [\boldsymbol{p}_r]_\times \end{bmatrix} \begin{bmatrix} \partial_{\boldsymbol{r}_P} H \\ \partial_{\boldsymbol{R}_\mathrm{v}} H \\ \boldsymbol{v}_P \\ \boldsymbol{\omega}_P \end{bmatrix},$$

where

$$\begin{bmatrix} \boldsymbol{p}_t \\ \boldsymbol{p}_r \end{bmatrix} = \begin{bmatrix} m\boldsymbol{I} & [\boldsymbol{s}]_\times^\top \\ [\boldsymbol{s}]_\times & \boldsymbol{J} \end{bmatrix} \begin{bmatrix} \boldsymbol{v}_P \\ \boldsymbol{\omega}_P \end{bmatrix}, \qquad \boldsymbol{p} = \boldsymbol{M}\boldsymbol{v}$$

The kinetic energy is then given by $H_\mathrm{kin} = \frac{1}{2}\boldsymbol{v}^\top \boldsymbol{M}\boldsymbol{v}$. This system can be written in standard pH form as $\dot{\boldsymbol{x}} = \boldsymbol{J}(\boldsymbol{x})\partial_{\boldsymbol{x}} H$.

4 Discretization procedure

A finite-element based technique to obtain a finite-dimensional pH system is illustrated. This methodology relies on the results explained in [9] and ahead, used in [6,7]. The essential feature of this method is that it is structure-preserving. Given the lossless, passive infinite-dimensional system (15), it allows obtaining a finite-dimensional representation that is again lossless and passive. The procedure boils down to three simple steps

1. The system is written in weak form;
2. An integration by parts is applied to highlight the proper boundary control;
3. A Galerkin method is employed to obtain a finite-dimensional system.

4.1 Illustration for the Elastodynamics PDE

To explain the methodology consider the elastodynamics PDE

$$\rho \frac{\partial^2 \boldsymbol{u}}{\partial t^2} - \mathrm{Div}\left(\boldsymbol{\mathcal{D}}\,\mathrm{Grad}(\boldsymbol{u})\right) = \boldsymbol{u}_d,$$

where a distributed control $\boldsymbol{u}_d$ (a volumetric force) is considered. This model describe the flexible vibrations assuming small deformations. It is embedded in the general formulation (12) and therefore the procedure explained here is easily adapted to the general formulation.
To get a pH representation the energy variables have to properly selected by considering the total energy

$$H = \frac{1}{2}\int_\Omega \left\{ \rho \left(\frac{\partial \boldsymbol{u}}{\partial t}\right)^2 + \boldsymbol{\Sigma} : \boldsymbol{\varepsilon} \right\} \mathrm{d}\Omega. \tag{20}$$

Taking as energy variables the linear momentum and the deformation

$$\begin{aligned} &\text{Energies} \quad \boldsymbol{x}_1 = \rho\, \partial_t \boldsymbol{u}, && \boldsymbol{X}_2 = \boldsymbol{\varepsilon} = \mathrm{Grad}(\boldsymbol{u}). \\ &\text{Co-energies} \quad \boldsymbol{e}_1 := \frac{\delta H}{\delta \boldsymbol{x}_1} = \partial_t \boldsymbol{u}, && \boldsymbol{E}_2 := \frac{\delta H}{\delta \boldsymbol{X}_2} = \boldsymbol{\Sigma}, \end{aligned} \tag{21}$$

the port-Hamiltonian representation in co-energy variables becomes

$$\underbrace{\begin{bmatrix}\rho & 0 \\ 0 & \boldsymbol{\mathcal{D}}^{-1}\end{bmatrix}}_{\boldsymbol{\mathcal{M}}} \frac{\partial}{\partial t} \begin{bmatrix}\boldsymbol{e}_1 \\ \boldsymbol{E}_2\end{bmatrix} = \underbrace{\begin{bmatrix}0 & \mathrm{Div} \\ \mathrm{Grad} & 0\end{bmatrix}}_{\boldsymbol{\mathcal{J}}} \begin{bmatrix}\boldsymbol{e}_1 \\ \boldsymbol{E}_2\end{bmatrix} + \underbrace{\begin{bmatrix}\boldsymbol{I} \\ 0\end{bmatrix}}_{\boldsymbol{\mathcal{B}}_d} \boldsymbol{u}_d$$

The interconnection operator may be decomposed as $\boldsymbol{\mathcal{J}} = \boldsymbol{\mathcal{J}}_{\mathrm{Div}} + \boldsymbol{\mathcal{J}}_{\mathrm{Grad}}$

$$\underbrace{\begin{bmatrix}0 & \mathrm{Div} \\ \mathrm{Grad} & 0\end{bmatrix}}_{\boldsymbol{\mathcal{J}}} = \underbrace{\begin{bmatrix}0 & \mathrm{Div} \\ 0 & 0\end{bmatrix}}_{\boldsymbol{\mathcal{J}}_{\mathrm{Div}}} + \underbrace{\begin{bmatrix}0 & 0 \\ \mathrm{Grad} & 0\end{bmatrix}}_{\boldsymbol{\mathcal{J}}_{\mathrm{Grad}}} \tag{22}$$

Assuming a Neumann boundary conditions (the normal traction $\boldsymbol{\tau}$ is known at the boundary), this system can be written compactly as a boundary control system

$$\begin{aligned}\boldsymbol{\mathcal{M}} \frac{\partial \boldsymbol{e}}{\partial t} &= \boldsymbol{\mathcal{J}} \boldsymbol{e} + \boldsymbol{\mathcal{B}}_d \boldsymbol{u}_d, \\ \boldsymbol{y}_d &= \boldsymbol{\mathcal{B}}_d^* \boldsymbol{e}, \\ \boldsymbol{u}_\partial &= [\boldsymbol{E}_2 \cdot \boldsymbol{n}|_{\Gamma_N},\ \boldsymbol{e}_1|_{\Gamma_D}], \\ \boldsymbol{y}_\partial &= [\boldsymbol{e}_1|_{\Gamma_N},\ \boldsymbol{E}_2 \cdot \boldsymbol{n}|_{\Gamma_D}].\end{aligned} \tag{23}$$

The system is defined over the state space

$$\mathscr{X} = \mathscr{L}^2(\Omega, \mathbb{R}^3) \times \mathscr{L}^2(\Omega, \mathbb{R}^{3\times 3}_{\mathrm{sym}}),$$

where $\mathscr{L}^2$ is the space of square integrable functions. Taking $[\boldsymbol{a}, \boldsymbol{A}],\ [\boldsymbol{b}, \boldsymbol{B}] \in \mathscr{X}$ the inner product is computed as

$$\langle [\boldsymbol{a}, \boldsymbol{A}],\ [\boldsymbol{b}, \boldsymbol{B}] \rangle_{\mathscr{X}} = \int_\Omega \boldsymbol{a} \cdot \boldsymbol{b} \,\mathrm{d}\Omega + \int_\Omega \boldsymbol{A} : \boldsymbol{B} \,\mathrm{d}\Omega.$$

The total energy is then computed as an inner product modulated by the mass operator $H = \frac{1}{2} \langle \boldsymbol{e},\ \boldsymbol{\mathcal{M}} \boldsymbol{e} \rangle_{\mathscr{X}}$ (see (20)). The power balance is computed by applied the Stokes theorem (18)

$$\dot{H} = \langle \boldsymbol{e}, \boldsymbol{\mathcal{M}} \partial_t \boldsymbol{e} \rangle_{\mathscr{X}} = \langle \boldsymbol{y}_\partial, \boldsymbol{u}_\partial \rangle_{\mathscr{L}^2(\partial\Omega, \mathbb{R}^3)} + \langle \boldsymbol{y}_d, \boldsymbol{u}_d \rangle_{\mathscr{L}^2(\Omega, \mathbb{R}^3)}. \tag{24}$$

So the system is lossless and passive with storage function given by the total energy. Considering a test function $\boldsymbol{w} = [\boldsymbol{w}_1,\ \boldsymbol{W}_2]$ the weak form reads

$$\langle \boldsymbol{w},\ \boldsymbol{\mathcal{M}}\ \partial_t \boldsymbol{e} \rangle_{\mathscr{X}} = \langle \boldsymbol{w},\ \boldsymbol{\mathcal{J}} \boldsymbol{e} \rangle_{\mathscr{X}} + \langle \boldsymbol{w},\ \boldsymbol{\mathcal{B}}_d \boldsymbol{u}_d \rangle_{\mathscr{X}}$$

The bilinear form $m(\boldsymbol{w}, \partial_t \boldsymbol{e}) = \langle \boldsymbol{w},\ \boldsymbol{\mathcal{M}}\ \partial_t \boldsymbol{e} \rangle_{\mathscr{X}}$ is symmetric and coercive. The bilinear form $b_d(\boldsymbol{w}, \boldsymbol{u}_d) := \langle \boldsymbol{w},\ \boldsymbol{\mathcal{B}}_d \boldsymbol{u}_d \rangle_{\mathscr{X}}$ takes into account distributed control. Now an integration by parts is applied on $\boldsymbol{\mathcal{J}}_{\mathrm{Div}}$:

$$\langle \boldsymbol{w},\ \boldsymbol{\mathcal{J}} \boldsymbol{e} \rangle_{\mathscr{X}} = \langle \boldsymbol{w},\ \boldsymbol{\mathcal{J}}_{\mathrm{Grad}} \boldsymbol{e} \rangle_{\mathscr{X}} - \langle \boldsymbol{\mathcal{J}}_{\mathrm{Grad}} \boldsymbol{w},\ \boldsymbol{e} \rangle_{\mathscr{X}} + \langle \boldsymbol{w},\ \boldsymbol{u}_\partial \rangle_{\mathscr{L}^2(\partial\Omega)}. \tag{25}$$

The expression $j_{\mathrm{Grad}}(\boldsymbol{w}, \boldsymbol{e}) := \langle \boldsymbol{w},\ \boldsymbol{\mathcal{J}}_{\mathrm{Grad}} \boldsymbol{e} \rangle_{\mathscr{X}} - \langle \boldsymbol{\mathcal{J}}_{\mathrm{Grad}} \boldsymbol{w},\ \boldsymbol{e} \rangle_{\mathscr{X}}$ is a skew symmetric bilinear form as it holds $j_{\mathrm{Grad}}(\boldsymbol{w}, \boldsymbol{e}) = -j_{\mathrm{Grad}}(\boldsymbol{e}, \boldsymbol{w})$. The bilinear form $b_\partial(\boldsymbol{w}, \boldsymbol{u}_\partial) := \langle \boldsymbol{w},\ \boldsymbol{u}_\partial \rangle_{\mathscr{L}^2(\partial\Omega)}$ imposes the Neumann condition weakly. System (23) is now rewritten in weak form

$$m(\boldsymbol{w}, \partial_t \boldsymbol{e}) = j_{\mathrm{Grad}}(\boldsymbol{w}, \boldsymbol{e}) + b_d(\boldsymbol{w}, \boldsymbol{u}_d) + b_\partial(\boldsymbol{w}, \boldsymbol{u}_\partial). \tag{26}$$

In this formulation the Dirichlet boundary condition have to be imposed strongly. For this reason the test function will belong to

$$
\begin{aligned}
&\boldsymbol{w}_1 \in \mathscr{H}^1_{\Gamma_D}(\Omega, \mathbb{R}^3) := \{\boldsymbol{w}_1 \in \mathscr{H}^1(\Omega, \mathbb{R}^d) |\ \boldsymbol{w}_1|_{\Gamma_D} = 0\}, \\
&\boldsymbol{W}_2 \in \mathscr{L}^2(\Omega, \mathbb{R}^{3\times 3}_{\text{sym}}),
\end{aligned}
$$

where $\mathscr{H}^1$ is the space of square integrable functions whose gradient is square integrable. The output equation is discretized considering test function $\boldsymbol{w}_\partial$ defined over the boundary

$$
\langle \boldsymbol{w}_\partial,\ \boldsymbol{y}_\partial \rangle_{\mathscr{X}} = \langle \boldsymbol{w}_\partial,\ \boldsymbol{e}_1 \rangle_{\mathscr{X}}\,. \tag{27}
$$

If a Galerkin method is applied then corresponding test and trial functions are discretized using the same basis

$$
\begin{aligned}
\boldsymbol{w}_1(\boldsymbol{x}, t) &= \boldsymbol{\phi}_1(\boldsymbol{x})^\top \mathbf{w}_1(t), \qquad & \boldsymbol{W}_2(\boldsymbol{x}, t) &= \boldsymbol{\phi}_2(\boldsymbol{x})^\top \mathbf{w}_2(t), \\
\boldsymbol{e}_1(\boldsymbol{x}, t) &= \boldsymbol{\phi}_1(\boldsymbol{x})^\top \mathbf{e}_1(t), \qquad & \boldsymbol{E}_2(\boldsymbol{x}, t) &= \boldsymbol{\phi}_2(\boldsymbol{x})^\top \mathbf{e}_2(t),
\end{aligned}
$$

where the bold italic variables represent numerical vectors. A finite dimensional pH system is readily obtained

$$
\begin{aligned}
\mathbf{M}\dot{\mathbf{e}} &= \mathbf{J}\mathbf{e} + \mathbf{B}_d \mathbf{u}_d + \mathbf{B}_\partial \mathbf{u}_\partial, \\
\mathbf{y}_d &:= \mathbf{M}_d \widetilde{\mathbf{y}}_d = \mathbf{B}_d^\top \mathbf{e}, \\
\mathbf{y}_\partial &:= \mathbf{M}_\partial \widetilde{\mathbf{y}}_\partial = \mathbf{B}_\partial^\top \mathbf{e}.
\end{aligned} \tag{28}
$$

It is important to notice that this system is again lossless and passive. The discrete energy is $H_d = \frac{1}{2}\mathbf{e}^\top \mathbf{M}\mathbf{e}$. The discrete power balance is given by

$$
\dot{H}_d = \mathbf{e}^\top \mathbf{M}\dot{\mathbf{e}} = \mathbf{e}^\top (\mathbf{J}\dot{\mathbf{e}} + \mathbf{B}_d \mathbf{u}_d + \mathbf{B}_\partial \mathbf{u}_\partial) = \mathbf{y}_d^\top \mathbf{u}_d + \mathbf{y}_\partial^\top \mathbf{u}_\partial
$$

Remark 4 Vectors $\widetilde{\mathbf{y}}_d, \widetilde{\mathbf{y}}_\partial$ correspond to the output degrees of freedom. The outputs $\mathbf{y}_d, \mathbf{y}_\partial$ have been defined incorporating the mass matrix in order get the discrete power balance $\dot{H}_d = \mathbf{u}_\partial^\top \mathbf{y}_\partial + \mathbf{u}_d^\top \mathbf{y}_d$.

Remark 5 Stable mixed finite elements for the elastodynamics problem are detailed in [3]. The formulation therein is based on a weak form obtained by integration by parts of the $\boldsymbol{\mathcal{J}}_{\text{Grad}}$ operator. The mixed finite element method for such a problem are then stable in the sense of Brezzi thanks to the properties of L^2/H^{Div} finite element spaces. However, the discretization scheme proposed here allows for an easier representation of floating bodies as the free condition corresponds to zero Neumann boundary conditions.

4.2 Discretized rigid-flexible port-Hamiltonian dynamics

The same methodology is applied to system (15). If corresponding test functions w, state e and the effort functions z are discretized using the same bases

$$
\boldsymbol{w}(\boldsymbol{x}, t) = \boldsymbol{\phi}(\boldsymbol{x})^\top \mathbf{w}(t), \quad \boldsymbol{e}(\boldsymbol{x}, t) = \boldsymbol{\phi}(\boldsymbol{x})^\top \mathbf{e}(t), \quad \boldsymbol{z}(\boldsymbol{x}, t) = \boldsymbol{\phi}(\boldsymbol{x})^\top \mathbf{z}(t),
$$

then a finite-dimensional pHDAE system is obtained (after integration by parts of the $\mathcal{J}_{\mathrm{Div}}$ operator)

$$\begin{aligned} \mathbf{E}(\mathbf{e})\dot{\mathbf{e}} &= \mathbf{J}(\mathbf{e})\mathbf{z}(\mathbf{e}) + \mathbf{B}_d(\mathbf{e})\mathbf{u}_d + \mathbf{B}_\partial(\mathbf{e})\mathbf{u}_\partial, \\ \mathbf{y}_d &:= \mathbf{M}_d\widetilde{\mathbf{y}}_d = \mathbf{B}_d^\top \mathbf{z}(\mathbf{e}), \\ \mathbf{y}_\partial &:= \mathbf{M}_\partial\widetilde{\mathbf{y}}_\partial = \mathbf{B}_\partial^\top \mathbf{z}(\mathbf{e}). \end{aligned} \tag{29}$$

The computation of vector $\mathbf{z}$ is based on the discrete Hamiltonian gradient:

$$\frac{\partial H_d}{\partial \mathbf{e}} = \mathbf{E}^\top \mathbf{z}, \qquad H_d = H_{d,\mathrm{kin}} + H_{d,\mathrm{def}} + H_{d,\mathrm{pot}},$$

This relation represents the finite-dimensional counterpart of (16). For the deformation and kinetic energy it is straightforward to find the link between the state and effort functions since those energies are quadratic in the state variable:

$$H_{d,\mathrm{kin}} + H_{d,\mathrm{def}} = \frac{1}{2}\mathbf{e}_{\mathrm{kd}}^\top \mathbf{M}_{\mathrm{kd}}\, \mathbf{e}_{\mathrm{kd}} \longrightarrow \mathbf{z}_{\mathrm{kd}} = \mathbf{e}_{\mathrm{kd}}, \tag{30}$$

where $\mathbf{e}_{\mathrm{kd}} = [\mathbf{v}_P;\, \boldsymbol{\omega}_P;\, \mathbf{v}_f;\, \boldsymbol{\Sigma}]$ and $\mathbf{M}_{\mathrm{kd}}$ is the discretization of the mass operator $\boldsymbol{\mathcal{M}}$ given in Eq (10). The only term that requires additional care is the potential energy and particularly the variational derivative of the Hamiltonian with respect to the deformation displacement $\boldsymbol{z}_u = \delta_{\boldsymbol{u}_f} H$. Consider the continuous power balance associate to

$$\dot{H} = \int_\Omega \frac{\partial \boldsymbol{u}_f}{\partial t} \cdot \boldsymbol{z}_u \,\mathrm{d}\Omega = \int_\Omega \frac{\partial \boldsymbol{u}_f}{\partial t} \cdot \frac{\delta H}{\delta \boldsymbol{u}_f} \,\mathrm{d}\Omega$$

The deformation velocity and its corresponding effort variable are discretized using the same basis, i.e. $\boldsymbol{u}_f = \boldsymbol{\phi}_u^\top \mathbf{u}_f$, $\boldsymbol{z}_u = \boldsymbol{\phi}_u^\top \mathbf{z}_u$. The discrete Hamiltonian rate assumes two equivalent expressions

$$\dot{H}_d(\mathbf{u}_f) = \begin{cases} \dot{\mathbf{u}}_f^\top \mathbf{M}_u\, \mathbf{z}_u, \\ \dot{\mathbf{u}}_f^\top \dfrac{\partial H_d}{\partial \mathbf{u}_f}, \end{cases}$$

where $\mathbf{M}_u = \int_\Omega \boldsymbol{\phi}_u\, \boldsymbol{\phi}_u^\top \,\mathrm{d}\Omega$. To preserve the power balance at a discrete level it must hold $\mathbf{z}_u = \mathbf{M}_u^{-1} \frac{\partial H_d}{\partial \mathbf{u}_f}$.

Remark 6 The set Γ_D for the Dirichlet condition has to be non empty cause otherwise the deformation field is allowed for rigid movement leading to a singular mass matrix.

4.3 Application to thin planar beams

If a thin planar flexible beams is considered as mechanical model. P is placed at the origin of the local frame $P = \{x = 0\}$, while C is the ending point of the beam $C = \{x = L\}$ (see Fig. 2). The beam has length L, Young modulus E, density

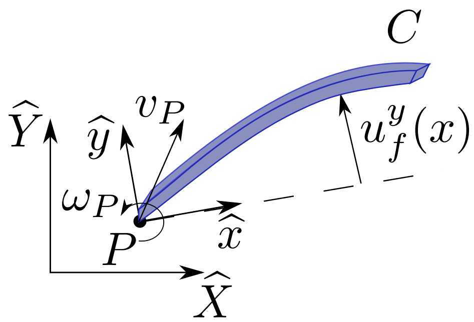

Fig. 2 Floating beam. The rigid motion is located at point P

ρ, cross section A and second moment of area I. The model in strong form for a flexible beam is then written compactly as

$$
\begin{aligned}
\begin{bmatrix} \boldsymbol{I} & 0 \\ 0 & \boldsymbol{\mathcal{M}} \end{bmatrix} \begin{bmatrix} \dot{\boldsymbol{q}} \\ \dot{\boldsymbol{p}} \end{bmatrix} &= \begin{bmatrix} 0 & \boldsymbol{\mathcal{J}}_{qe} \\ -\boldsymbol{\mathcal{J}}_{qe}^* & \boldsymbol{\mathcal{J}}_{e} \end{bmatrix} \begin{bmatrix} \partial_{\boldsymbol{q}} H \\ \boldsymbol{p} \end{bmatrix} + \begin{bmatrix} 0 \\ \boldsymbol{\mathcal{B}}_r \end{bmatrix} \boldsymbol{u}_\partial, \\
\boldsymbol{u}_\partial &= \boldsymbol{\mathcal{B}}_\partial \boldsymbol{p}, \\
\boldsymbol{y}_\partial &= \boldsymbol{\mathcal{C}}_\partial \boldsymbol{p},
\end{aligned} \tag{31}
$$

The state and boundary vectors are expressed as

$$
\begin{aligned}
\boldsymbol{q} &= \left[{}^i\boldsymbol{r}_P, \ \boldsymbol{R}_{\mathrm{v}}, \ \boldsymbol{u}_f\right]^\top \\
\boldsymbol{p} &= \left[v_P^x, \ v_P^y, \ \omega_P^z, \ v_f^x, \ v_f^y, \ n_x, \ m_x\right]^\top, \\
\boldsymbol{u}_\partial &= \left[F_P^x, \ F_P^y, \ T_P^z, \ F_C^x, \ F_C^y, \ T_C^z\right]^\top, \\
\boldsymbol{y}_\partial &= \left[v_P^x, \ v_P^y, \ \omega_P^z, \ v_C^x, \ v_C^y, \ \omega_C^z\right]^\top.
\end{aligned}
$$

The state contains the generalized coordinates $\boldsymbol{q}$, the linear and angular velocity $v_P^x, \ v_P^y, \ \omega_P^z$ at point P, the deformation velocity $v_f^x, \ v_f^y$ and the traction and bending stress $n_x, \ m_x$. The boundary input contains the forces and torques acting at the extremities of the beam, while the boundary output contains the velocities at the extremities of the beam. The deformation field has to be constrained, to prevent rigid movement (see Rmk. 6). The appropriate selection of the boundary condition for the deformation field is an avoidable problem that depends on the particular problem under consideration. Depending on the application, cantilever or simply supported boundary conditions may be considered (see Sec. §6)

$$
\text{Cantilever} \begin{cases} u_f^x(x=0) = 0, \\ u_f^y(x=0) = 0, \\ \partial_x u_f^y(x=0) = 0, \end{cases} \qquad \text{Simply supported} \begin{cases} u_f^x(x=0) = 0, \\ u_f^y(x=0) = 0, \\ u_f^y(x=L) = 0, \end{cases}
$$

Partitioning the $\boldsymbol{p}$ vector into rigid $\boldsymbol{p}_r = [v_P^x,\ v_P^y,\ \omega_P^z]^\top$ and flexible part $\boldsymbol{p}_f = [v_f^x,\ v_f^y,\ n_x,\ m_x]^\top$, the mass operator then is formulated as follows

$$\boldsymbol{\mathcal{M}} = \left[\begin{array}{c|c} \boldsymbol{\mathcal{M}}_{rr} & \boldsymbol{\mathcal{M}}_{rf} \\ \hline \boldsymbol{\mathcal{M}}_{fr} & \boldsymbol{\mathcal{M}}_{ff} \end{array}\right] = \left[\begin{array}{ccc|cccc} m & 0 & 0 & \mathcal{I}_\rho^L & 0 & 0 & 0 \\ 0 & m & s^x & 0 & \mathcal{I}_\rho^L & 0 & 0 \\ 0 & s^x & J^{zz} & 0 & \mathcal{I}_{\rho x}^L & 0 & 0 \\ \hline (\mathcal{I}_\rho^L)^* & 0 & 0 & \rho A & 0 & 0 & 0 \\ 0 & (\mathcal{I}_\rho^L)^* & (\mathcal{I}_{\rho x}^L)^* & 0 & \rho A & 0 & 0 \\ 0 & 0 & 0 & 0 & 0 & EA^{-1} & 0 \\ 0 & 0 & 0 & 0 & 0 & 0 & EI^{-1} \end{array}\right], \tag{32}$$

where $s^x = \int_0^L \rho A x \,\mathrm{d}x$ is the static moment, $J^{zz} = \int_0^L \rho A x^2 \,\mathrm{d}x$ is the moment of inertia, $\mathcal{I}_\rho^L := \int_0^L \rho A(\cdot)\,\mathrm{d}x$, $\mathcal{I}_{\rho x}^L := \int_0^L \rho A x(\cdot)\,\mathrm{d}x$. The interconnection operator is found by adapting the cross product to th planar case:

$$\boldsymbol{\mathcal{J}}_e(\boldsymbol{e}) = \left[\begin{array}{c|c} \boldsymbol{\mathcal{J}}_{rr} & \boldsymbol{\mathcal{J}}_{rf} \\ \hline \boldsymbol{\mathcal{J}}_{fr} & \boldsymbol{\mathcal{J}}_{ff} \end{array}\right] = \left[\begin{array}{ccc|cccc} 0 & 0 & +\widetilde{p}_t^y & 0 & 0 & 0 & 0 \\ 0 & 0 & -\widetilde{p}_t^x & 0 & 0 & 0 & 0 \\ -\widetilde{p}_t^y & +\widetilde{p}_t^x & 0 & -\mathcal{I}_{p_f^y}^L & +\mathcal{I}_{p_f^x}^L & 0 & 0 \\ \hline 0 & 0 & +(\mathcal{I}_{p_f^y}^L)^* & 0 & 0 & \partial_x & 0 \\ 0 & 0 & -(\mathcal{I}_{p_f^x}^L)^* & 0 & 0 & 0 & -\partial_{xx} \\ 0 & 0 & 0 & \partial_x & 0 & 0 & 0 \\ 0 & 0 & 0 & 0 & \partial_{xx} & 0 & 0 \end{array}\right] \tag{33}$$

where $\widetilde{p}_t^x, \widetilde{p}_t^y$ are the modified canonical momenta components (see (13)), $\mathcal{I}_{p_f^x}^L := \int_0^L \left\{2p_f^x + \rho A v_f^x\right\}(\cdot)\,\mathrm{d}x$ and $\mathcal{I}_{p_f^y}^L := \int_0^L \left\{2p_f^y + \rho A v_f^y\right\}(\cdot)\,\mathrm{d}x$. The control operators read

$$\boldsymbol{\mathcal{B}}_r = \begin{bmatrix} \boldsymbol{I}_{3\times 3} & \boldsymbol{\tau}_{CP}^\top \\ 0_{4\times 3} & 0_{4\times 3} \end{bmatrix} \qquad \text{with} \quad \boldsymbol{\tau}_{CP} = \begin{bmatrix} 1 & 0 & 0 \\ 0 & 1 & L \\ 0 & 0 & 1 \end{bmatrix}. \tag{34}$$

The discretization procedure detailed in §4 is extended to this case, considering that the differential operators here are

$$\boldsymbol{\mathcal{J}}_{\mathrm{Div}} = \begin{bmatrix} 0 & 0 & \partial_x & 0 \\ 0 & 0 & 0 & -\partial_{xx} \\ 0 & 0 & 0 & 0 \\ 0 & 0 & 0 & 0 \end{bmatrix}, \qquad \boldsymbol{\mathcal{J}}_{\mathrm{Grad}} = \begin{bmatrix} 0 & 0 & 0 & 0 \\ 0 & 0 & 0 & 0 \\ \partial_x & 0 & 0 & 0 \\ 0 & \partial_{xx} & 0 & 0 \end{bmatrix}.$$

This two operator play the same role as their previously defined homonyms. The 2 PDEs associated to the first and second line of $\boldsymbol{\mathcal{J}}_{\mathrm{Div}}$ are integrated by parts once and twice respectively, so that the boundary forces and momenta are naturally included in the discretized system as inputs. The finite-dimensional system then reads

$$\begin{aligned} \begin{bmatrix} \mathbf{I} & 0 & 0 \\ 0 & \mathbf{M}_{rr} & \mathbf{M}_{rf} \\ 0 & \mathbf{M}_{fr} & \mathbf{M}_{ff} \end{bmatrix} \begin{bmatrix} \dot{\mathbf{q}} \\ \dot{\mathbf{p}}_r \\ \dot{\mathbf{p}}_f \end{bmatrix} &= \begin{bmatrix} 0 & \mathbf{J}_{qr}(\mathbf{q}) & \mathbf{J}_{qf} \\ \mathbf{J}_{rq}(\mathbf{q}) & \mathbf{J}_{rr}(\mathbf{p}) & \mathbf{J}_{rf}(\mathbf{p}) \\ \mathbf{J}_{fq} & \mathbf{J}_{fr}(\mathbf{p}) & \mathbf{J}_{ff} \end{bmatrix} \begin{bmatrix} \partial_{\mathbf{q}} H \\ \mathbf{p}_r \\ \mathbf{p}_f \end{bmatrix} + \begin{bmatrix} 0 \\ \mathbf{B}_r \\ \mathbf{B}_f \end{bmatrix} \mathbf{u}_\partial, \\ \mathbf{y}_\partial &= \begin{bmatrix} 0 & \mathbf{B}_r^\top & \mathbf{B}_f^\top \end{bmatrix} \begin{bmatrix} \mathbf{q} \\ \mathbf{p}_r \\ \mathbf{p}_f \end{bmatrix}, \end{aligned} \tag{35}$$

Matrix $\mathbf{B}_r = [\mathbf{I}_{3\times 3},\ \boldsymbol{\tau}_{CP}^\top]$ accounts for the effect of boundary forces to the rigid part. Matrix $\mathbf{B}_f$ is the result of the integration by parts

$$\mathbf{B}_f = \begin{bmatrix} 0_{n_f^{vx}\times 3} & \boldsymbol{\phi}_{v_f^x}(L) & 0_{n_f^{vx}} & 0_{n_f^{vx}} \\ 0_{n_f^{vy}\times 3} & 0_{n_f^{vy}} & \boldsymbol{\phi}_{v_f^y}(L) & \partial_x \boldsymbol{\phi}_{v_f^y}(L) \\ 0_{n_f^{\sigma x}\times 3} & 0_{n_f^{\sigma x}} & 0_{n_f^{\sigma x}} & 0_{n_f^{\sigma x}} \\ 0_{n_f^{\sigma y}\times 3} & 0_{n_f^{\sigma y}} & 0_{n_f^{\sigma y}} & 0_{n_f^{\sigma y}} \end{bmatrix},$$

where $\boldsymbol{\phi}_{v_f^x},\ \boldsymbol{\phi}_{v_f^y}$ are the shape function for v_f^x, v_f^y and $\boldsymbol{\phi}_{v_f^x}$. Fields v_f^x, v_f^y, n_x, m_x are approximated using $n_f^{vx}, n_f^{vy}, n_f^{\sigma x}, n_f^{\sigma y}$ degrees of freedom respectively. System (35) can be rewritten compactly as

$$\begin{aligned} \mathbf{E}\dot{\mathbf{e}} &= \mathbf{J}(\mathbf{e})\mathbf{z}(\mathbf{e}) + \mathbf{B}_\partial \mathbf{u}_\partial \\ \mathbf{y}_\partial &= \mathbf{B}_\partial^\top \mathbf{z} \end{aligned} \tag{36}$$

This model describes the motion of a flexible floating beam that undergoes small deformations.

5 Multibody systems in pH form

In Sections §3, §4 the pH formulation of a single flexible floating body in infinite- and finite-dimensional form were presented. The construction of a multibody system is accomplished by exploiting the modularity of the port-Hamiltonian framework. Each element of the system is interconnected to the others by means of classical pH interconnections.

5.1 Interconnections of pHDAE systems

Consider two geniric pHDAE systems of the form

$$\begin{cases} \mathbf{E}_i\dot{\mathbf{e}}_i = \mathbf{J}_i\mathbf{z}_i(\mathbf{e}_i) + \mathbf{B}_i^{\text{int}}\mathbf{u}_i^{\text{int}} + \mathbf{B}_i^{\text{ext}}\mathbf{u}_i^{\text{ext}} \\ \mathbf{y}_i^{\text{int}} = \mathbf{B}_i^{\text{int}\top}\mathbf{z}_i \\ \mathbf{y}_i^{\text{ext}} = \mathbf{B}_i^{\text{ext}\top}\mathbf{z}_i \end{cases} \qquad \forall i = 1, 2. \tag{37}$$

where $\partial_{\mathbf{e}_i} H_i = \mathbf{E}_i^\top \mathbf{z}_i$. Systems of this kind arise from the discretization of formulation (15). The interconnection uses the internal control $\mathbf{u}_i^{\text{int}}$. An interconnection is said to be power preserving if and only if the following holds:

$$\langle \mathbf{u}_1^{\text{int}},\ \mathbf{y}_1^{\text{int}}\rangle + \langle \mathbf{u}_2^{\text{int}},\ \mathbf{y}_2^{\text{int}}\rangle = 0. \tag{38}$$

The power going out from one system flows in the other in a lossless manner. Two main interconnections of this kind are of interest when coupling system: the gyrator and transformer interconnection.

Gyrator interconnection The gyrator interconnection reads

$$\mathbf{u}_1^{\text{int}} = -\mathbf{C}\mathbf{y}_2^{\text{int}}, \qquad \mathbf{u}_2^{\text{int}} = \mathbf{C}^\top \mathbf{y}_1^{\text{int}}.$$

This interconnection verifies (38). It is easy to verify that from this interconnection, it is obtained

$$\begin{bmatrix}\mathbf{E}_1 & 0\\ 0 & \mathbf{E}_2\end{bmatrix}\begin{bmatrix}\dot{\mathbf{e}}_1\\ \dot{\mathbf{e}}_2\end{bmatrix} = \begin{bmatrix}\mathbf{J}_1 & -\mathbf{B}_1^{\text{int}}\mathbf{C}\mathbf{B}_2^{\text{int}\top}\\ \mathbf{B}_2^{\text{int}}\mathbf{C}\mathbf{B}_1^{\text{int}\top} & \mathbf{J}_2\end{bmatrix}\begin{bmatrix}\mathbf{z}_1\\ \mathbf{z}_2\end{bmatrix} + \begin{bmatrix}\mathbf{B}_1^{\text{ext}} & 0\\ 0 & \mathbf{B}_2^{\text{ext}}\end{bmatrix}\begin{bmatrix}\mathbf{u}_1^{\text{ext}}\\ \mathbf{u}_2^{\text{ext}}\end{bmatrix}$$

$$\begin{bmatrix}\mathbf{y}_1^{\text{ext}}\\ \mathbf{y}_2^{\text{ext}}\end{bmatrix} = \begin{bmatrix}\mathbf{B}_1^{\text{ext}\top} & 0\\ 0 & \mathbf{B}_2^{\text{ext}\top}\end{bmatrix}\begin{bmatrix}\mathbf{z}_1\\ \mathbf{z}_2\end{bmatrix},$$

with $H(\mathbf{e}_1, \mathbf{e}_2) = H_1(\mathbf{e}_1) + H_2(\mathbf{e}_2)$.

Transformer interconnection The transformer interconnection reads

$$\mathbf{u}_1^{\text{int}} = -\mathbf{C}\mathbf{u}_2^{\text{int}}, \qquad \mathbf{y}_2^{\text{int}} = \mathbf{C}^\top \mathbf{y}_1^{\text{int}}.$$

Again, this interconnection verifies (38). After the interconnection the final system is differential algebraic:

$$\begin{bmatrix}\mathbf{E}_1 & 0 & 0\\ 0 & \mathbf{E}_2 & 0\\ 0 & 0 & 0\end{bmatrix}\begin{bmatrix}\dot{\mathbf{e}}_1\\ \dot{\mathbf{e}}_2\\ \dot{\boldsymbol{\lambda}}\end{bmatrix} = \begin{bmatrix}\mathbf{J}_1 & 0 & -\mathbf{B}_1^{\text{int}}\mathbf{C}\\ 0 & \mathbf{J}_2 & \mathbf{B}_2^{\text{int}}\\ \mathbf{C}^\top\mathbf{B}_1^{\text{int}\top} & -\mathbf{B}_2^{\text{int}\top} & 0\end{bmatrix}\begin{bmatrix}\mathbf{z}_1\\ \mathbf{z}_2\\ \boldsymbol{\lambda}\end{bmatrix} + \begin{bmatrix}\mathbf{B}_1^{\text{ext}} & 0\\ 0 & \mathbf{B}_2^{\text{ext}}\\ 0 & 0\end{bmatrix}\begin{bmatrix}\mathbf{u}_1^{\text{ext}}\\ \mathbf{u}_2^{\text{ext}}\end{bmatrix}$$

$$\begin{bmatrix}\mathbf{y}_1^{\text{ext}}\\ \mathbf{y}_2^{\text{ext}}\end{bmatrix} = \begin{bmatrix}\mathbf{B}_1^{\text{ext}\top} & 0 & 0\\ 0 & \mathbf{B}_2^{\text{ext}\top} & 0\end{bmatrix}\begin{bmatrix}\mathbf{z}_1\\ \mathbf{z}_2\\ \boldsymbol{\lambda}\end{bmatrix}.$$

5.2 Application to multibody systems of beams

Once a discretized system is obtained by application of a transformer interconnection lossless joints can be introduced. A common example is an hinged link between two beams. Consider the discretization (36). The boundary control input $\mathbf{u}_{\partial,i}$ may be split interconnection variables and external forcing $\mathbf{u}_{\partial,i} = [\mathbf{u}_i^{\text{int}};\ \mathbf{u}_i^{\text{ext}}]$. In this case the internal variables are

$$\begin{aligned}
\mathbf{u}_1^{\text{int}} &= [F_{C_1}^x,\, F_{C_1}^y]^\top := \mathbf{F}_{C_1}, &\qquad \mathbf{y}_1^{\text{int}} &= [v_{C_1}^x,\, v_{C_1}^y]^\top := \mathbf{v}_{C_1},\\
\mathbf{u}_2^{\text{int}} &= [F_{P_2}^x,\, F_{P_2}^y]^\top := \mathbf{F}_{P_2}, &\qquad \mathbf{y}_2^{\text{int}} &= [v_{P_2}^x,\, v_{P_2}^y]^\top := \mathbf{v}_{P_2}.
\end{aligned}$$

The interconnection matrix is the relative rotation matrix between the two local frames

$$\mathbf{R}(\theta) = \begin{bmatrix}\cos(\theta) & -\sin(\theta)\\ \sin(\theta) & \cos(\theta)\end{bmatrix}, \qquad \theta(t) = \theta(0) + \int_0^t (\omega_{P_2}^z - \omega_{P_1}^z)\, \mathrm{d}\tau. \tag{39}$$

The transformer interconnection

$$\mathbf{u}_1^{\text{int}} = -\mathbf{R}(\theta)\mathbf{u}_2^{\text{int}}, \qquad \mathbf{y}_2^{\text{int}} = \mathbf{R}(\theta)^\top \mathbf{y}_1^{\text{int}}, \tag{40}$$

imposes the constraints on a velocity level and gives rise to a quasi-linear index 2 pHDAE (see Appendix A for the index definition):

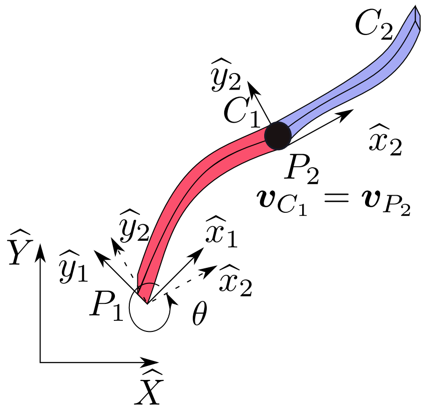

Fig. 3 Two beams interconnected by an hinge

$$
\begin{aligned}
&\begin{bmatrix} \mathbf{E}_1 & 0 & 0 \\ 0 & \mathbf{E}_2 & 0 \\ 0 & 0 & 0 \end{bmatrix} \begin{bmatrix} \dot{\mathbf{e}}_1 \\ \dot{\mathbf{e}}_2 \\ \dot{\boldsymbol{\lambda}} \end{bmatrix} = \begin{bmatrix} \mathbf{J}_1(\mathbf{e}_1) & 0 & -\mathbf{B}_1^{\mathrm{int}}\mathbf{R} \\ 0 & \mathbf{J}_2(\mathbf{e}_2) & \mathbf{B}_2^{\mathrm{int}} \\ \mathbf{R}^\top \mathbf{B}_1^{\mathrm{int}\top} & -\mathbf{B}_2^{\mathrm{int}\top} & 0 \end{bmatrix} \begin{bmatrix} \mathbf{z}_1 \\ \mathbf{z}_2 \\ \boldsymbol{\lambda} \end{bmatrix} + \begin{bmatrix} \mathbf{B}_{\partial 1}^{\mathrm{ext}} & 0 \\ 0 & \mathbf{B}_{\partial 2}^{\mathrm{ext}} \\ 0 & 0 \end{bmatrix} \begin{bmatrix} \mathbf{u}_1^{\mathrm{ext}} \\ \mathbf{u}_2^{\mathrm{ext}} \end{bmatrix} \\
&\qquad\qquad \begin{bmatrix} \mathbf{y}_1^{\mathrm{ext}} \\ \mathbf{y}_2^{\mathrm{ext}} \end{bmatrix} = \begin{bmatrix} \mathbf{B}_{\partial 1}^{\mathrm{ext}\top} & 0 & 0 \\ 0 & \mathbf{B}_{\partial 2}^{\mathrm{ext}\top} & 0 \end{bmatrix} \begin{bmatrix} \mathbf{z}_1 \\ \mathbf{z}_2 \\ \boldsymbol{\lambda} \end{bmatrix}.
\end{aligned}
\tag{41}
$$

A transformer interconnection is indeed equivalent to a gyrator interconnection of pHDAE systems. It is sufficient to interchange the role of output and input of the second system $\mathbf{u}_2^{\mathrm{int}} \leftrightarrow \mathbf{y}_2^{\mathrm{int}}$. The output than plays the role of a Lagrange multiplier. To illustrate this idea, consider the discretization of the second planar beam system (36), where the input $\mathbf{u}_2^{\mathrm{int}}$ is now considered as Lagrange multiplier $\boldsymbol{\lambda}_2$ and the output $\mathbf{y}_2^{\mathrm{int}}$ plays the role of $\mathbf{u}_2^{\mathrm{int}}$. The discretized system assumes the following differential-algebraic structure

$$
\begin{aligned}
\begin{bmatrix} \mathbf{E}_2 & 0 \\ 0 & 0 \end{bmatrix} \begin{bmatrix} \dot{\mathbf{e}}_2 \\ \dot{\boldsymbol{\lambda}}_2 \end{bmatrix} &= \begin{bmatrix} \mathbf{J}_2(\mathbf{e}_2) & \mathbf{B}_2^{\mathrm{int}} \\ -\mathbf{B}_2^{\mathrm{int}\top} & 0 \end{bmatrix} \begin{bmatrix} \mathbf{z}_2 \\ \boldsymbol{\lambda}_2 \end{bmatrix} + \begin{bmatrix} 0 \\ \mathbf{I} \end{bmatrix} \mathbf{u}_2^{\mathrm{int}} + \begin{bmatrix} \mathbf{B}_2^{\mathrm{ext}} \\ 0 \end{bmatrix} \mathbf{u}_2^{\mathrm{ext}} \\
\mathbf{y}_2^{\mathrm{int}} &= \boldsymbol{\lambda}_2 \\
\mathbf{y}_2^{\mathrm{ext}} &= \mathbf{B}_2^{\mathrm{ext}\top} \mathbf{z}_2
\end{aligned}
\tag{42}
$$

This system represent an improper system. Now, the same hinged interconnection can be obtained using a gyrator interconnection

$$
\mathbf{u}_1^{\mathrm{int}} = -\mathbf{R}(\theta)\mathbf{y}_2^{\mathrm{int}}, \qquad \mathbf{u}_2^{\mathrm{int}} = \mathbf{R}(\theta)^\top \mathbf{y}_1^{\mathrm{int}}, \tag{43}
$$

The resulting differential-algebraic system is exactly (41), which is proper. The equivalence between the two representation is represented in Fig. 4. This approach allows the modular construction of systems of arbitrary complexity. Other kind of lossless joints (prismatic, spherical) can be modeled by appropriate interconnections. The system can then be simulated by using specific DAE solvers [5].

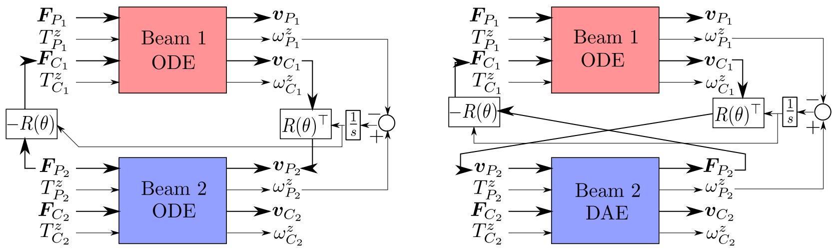

Fig. 4 Block diagrams representing the transformer interconnection (40) (left) and the equivalent gyrator interconnection (43) (right)

5.3 The linear case: sub-structuring and model reduction

If the angular velocities and the relative orientations are small then the system may be linearized about a particular geometrical configuration. Omitting the partition related to the generalized coordinates $\mathbf{q}$ and dividing the system into rigid and flexible dynamics, the resulting equations are then expressed as

$$\begin{bmatrix} \mathbf{M}_{rr} & \mathbf{M}_{rf} & 0 \\ \mathbf{M}_{fr} & \mathbf{M}_{ff} & 0 \\ 0 & 0 & 0 \end{bmatrix} \begin{bmatrix} \dot{\mathbf{p}}_r \\ \dot{\mathbf{p}}_f \\ \dot{\boldsymbol{\lambda}} \end{bmatrix} = \begin{bmatrix} 0 & 0 & \mathbf{G}_r^\top \\ 0 & \mathbf{J}_{ff} & \mathbf{G}_f^\top \\ -\mathbf{G}_r & -\mathbf{G}_f & 0 \end{bmatrix} \begin{bmatrix} \mathbf{p}_r \\ \mathbf{p}_f \\ \boldsymbol{\lambda} \end{bmatrix} + \begin{bmatrix} \mathbf{B}_r \\ \mathbf{B}_f \\ 0 \end{bmatrix} \mathbf{u}. \tag{44}$$

The Hamiltonian is now a quadratic function of the state variables $H = \frac{1}{2}\mathbf{p}^\top \mathbf{M}\mathbf{p}$ [4]. The modular construction of complex multi-body systems then is analogous to a sub-structuring technique [20] where the velocities and forces are linked at the interconnection points. Such system can be reduced using Krylov subspace method directly on the DAE formulation [14]. The basic idea relies on the construction of a subspace $\mathbf{V}_f^{\text{red}}$ for the vector $\mathbf{p}_f$ such that $\mathbf{p}_f \approx \mathbf{V}_f^{\text{red}}\mathbf{p}_f^{\text{red}}$. The reduced system then reads

$$\begin{bmatrix} \mathbf{M}_{rr} & \mathbf{M}_{rf}^{\text{red}} & 0 \\ \mathbf{M}_{fr}^{\text{red}} & \mathbf{M}_{ff}^{\text{red}} & 0 \\ 0 & 0 & 0 \end{bmatrix} \begin{bmatrix} \dot{\mathbf{p}}_r \\ \dot{\mathbf{p}}_f^{\text{red}} \\ \dot{\lambda} \end{bmatrix} = \begin{bmatrix} 0 & 0 & \mathbf{G}_r^\top \\ 0 & \mathbf{J}_{ff}^{\text{red}} & \mathbf{G}_f^{\text{red}\top} \\ -\mathbf{G}_r & -\mathbf{G}_f^{\text{red}} & 0 \end{bmatrix} \begin{bmatrix} \mathbf{p}_r \\ \mathbf{p}_f^{\text{red}} \\ \lambda \end{bmatrix} + \begin{bmatrix} \mathbf{B}_r \\ \mathbf{B}_f^{\text{red}} \\ 0 \end{bmatrix} \mathbf{u}, \tag{45}$$

where the second row has been pre-multiplied by $\mathbf{V}_f^{\text{red}\top}$. Alternatively, a null space matrix can employed to eliminate the Lagrange multiplier and preserve the port-Hamiltonian structure. Consider the pHDAE (44) where the differential and algebraic part are explicitly separated

$$\begin{aligned} \mathbf{M}\dot{\mathbf{p}} &= \mathbf{J}\mathbf{p} + \mathbf{G}^\top \boldsymbol{\lambda} + \mathbf{B}\mathbf{u}, \\ 0 &= \mathbf{G}\mathbf{p}, \end{aligned} \tag{46}$$

and a matrix $\mathbf{P}$ that satisfies

$$\text{range}\{\mathbf{P}\} = \text{null}\{\mathbf{G}\},$$

then the admissible variable belongs to the range of $\mathbf{P}$, considering the transformation $\widehat{\mathbf{p}} = \mathbf{P}\mathbf{p}$ and pre-multiplying the system by $\mathbf{P}^\top$ an equivalent ODE is obtained

$$\widehat{\mathbf{M}}\, \dot{\widehat{\mathbf{p}}} = \widehat{\mathbf{J}}\, \widehat{\mathbf{p}} + \widehat{\mathbf{B}}\, \mathbf{u},$$

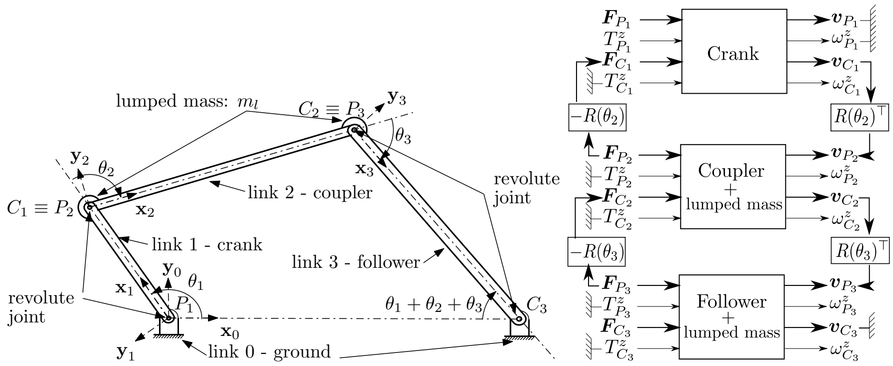

Fig. 5 Four bar mechanism illustration (left, taken from [12]) and block diagram used for the eigenvalues analysis (right)

with $\widehat{\mathbf{M}} = \mathbf{P}^\top \mathbf{M}\mathbf{P}$, $\widehat{\mathbf{J}} = \mathbf{P}^\top \mathbf{J}\mathbf{P}$, $\widehat{\mathbf{B}} = \mathbf{P}^\top \mathbf{B}$. The actual computation of $\mathbf{P}$ can be obtained by QR decomposition of matrix $\mathbf{G}$ [21]. A pH system in standard form is then obtained considering the variable change $\widehat{\mathbf{x}} = \widehat{\mathbf{M}}\widehat{\mathbf{p}}$

$$\dot{\widehat{\mathbf{x}}} = \widehat{\mathbf{J}}\widehat{\mathbf{Q}}\,\widehat{\mathbf{x}} + \widehat{\mathbf{B}}\mathbf{u}, \qquad \widehat{\mathbf{Q}} := \widehat{\mathbf{M}}^{-1}$$

Once an equivalent ODE formulation is obtained the concepts and ideas presented in [11] can be used to reduce the flexible dynamics.

6 Validation

In this section numerical simulations are perform to assess the correctness of the proposed formulation. A first example corners the computation of eigenvalues of a four bar mechanics for different geometrical configuration. The second example is a rotating crank-slider. In this case the non-linearities cannot be neglected. The third example is a beam hinged and undergoing external excitations so that the out of plane motion becomes important. The following examples make use of Euler Bernoulli beam model (35). To discretize the system, Lagrange polynomial of order one are used for v_f^x and n_x, while Hermite polynomials are used for v_f^y and m_x. This choice ensures the conformity with respect to the differential operator. The Firedrake python library [29] is employed to construct the finite-dimensional discretization.

6.1 Linear analysis of a four-bar mechanism

The four-bar mechanism has one degree of freedom and represents a closed chain of rigid body. The data are taken from [19,12] are recalled in Table 1. In Fig. 5 the mechanism and the corresponding block diagram used for constructing the final pH system are presented. The lumped mass are directly included in the coupler and follower model considering a simple modification to the rigid mass matrix

$$\mathbf{M}_{rr}^{i+m_l}[1:2,1:2] = \mathbf{M}_{rr}^{i}[1:2,1:2] + \mathbf{I}_{2\times 2} m_l, \qquad (47)$$

Table 1 Four-bar mechanism links properties: each link is a uniform beam with mass density $\rho = 2714\,\mathrm{kg/m^3}$ and Young modulus $E = 7.1\,10^{10}\,\mathrm{N/m^2}$. The lumped masses $m_l = 0.042\,\mathrm{kg}$ are taken into account considering an additional mass at P for link 2 and 3.

i	0	1	2	3
Name	ground	crank	coupler	follower
Length L_i (m)	0.254	0.108	0.2794	0.2705
Cross section A_i (m^2)	–	$1.0774\,10^{-4}$	$4.0645\,10^{-5}$	$4.0645\,10^{-5}$
Flexural rigidity $(EI)_i$ (Nm^2)	–	11.472	0.616	0.616

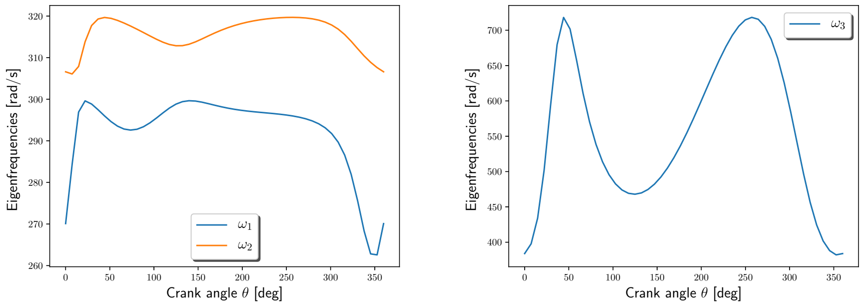

Fig. 6 Eigenvalues $\omega_i,\ i = 1, 2, 3$ for the four bar mechanism for varying crank angle.

where $i = 2, 3$ denotes the coupler or follower model. Given a certain crank angle θ_1 the relative angles between the different links are found by solving the two kinematic constraints

$$
\begin{aligned}
L_1 \cos(\theta_1) + L_2 \cos(\theta_1 + \theta_2) + L_3 \cos(\theta_1 + \theta_2 + \theta_3) &= L_0, \\
L_1 \sin(\theta_1) + L_2 \sin(\theta_1 + \theta_2) + L_3 \sin(\theta_1 + \theta_2 + \theta_3) &= 0.
\end{aligned}
$$

Once the angles describing the geometrical configuration are known, the transformer interconnection (40) is applied to insert a revolute joint between adjacent links. For the deformation field a cantilever condition is imposed for each beam. The resulting system is then constrained to ground by imposing to following equalities

$$
\mathbf{v}_{P_1} = 0, \quad \omega^z_{P_1} = 0, \quad \mathbf{v}_{C_3} = 0.
$$

The resulting system is expressed in pH form as $\mathbf{E}\dot{\mathbf{e}} = \mathbf{J}\mathbf{e}$. The eigenfrequencies are then found by solving the generalized eigenvalue problem $\mathbf{E}\boldsymbol{\Phi} = \mathbf{J}\boldsymbol{\Phi}\boldsymbol{\Lambda}$. Since $\mathbf{J}$ is skew-symmetric the eigenvalues will be imaginary $\boldsymbol{\lambda} = j\boldsymbol{\Omega}$. The first three pulsations are reported in Fig. 6 for different values of the crank angle θ_1. The results match perfectly [19, 12], assessing the validity of the linear model.

6.2 Rotating crank-slider

To verify the non-linear planar model a crank-slider rotating at high speed is considered. The example is retrieved form [15]. The crank is considered as rigid, with length $L_{\mathrm{cr}} = 0.15$ m and rotates at a constant angular rate $\omega_{\mathrm{cr}} = 150$ rad/s.

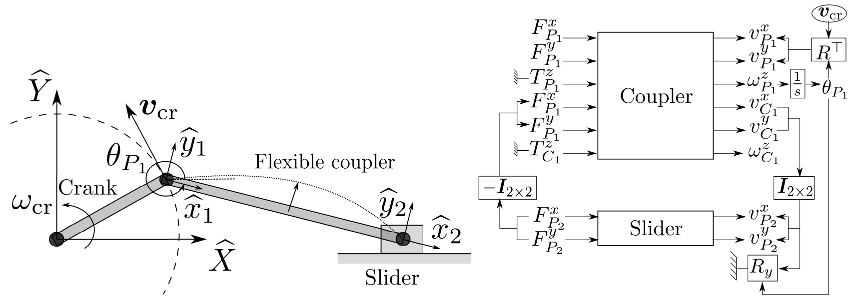

Fig. 7 Crank slider illustration (left) and block diagram (right)

The flexible coupler has length $L_{\rm cl} = 0.3$ [m] and a circular cross section whose diameter is $d_{\rm cl} = 6$ mm. Its Young modulus and density are given by $E_{\rm cl} = 0.2\ 10^{12}$ Pa, $\rho_{\rm cl} = 7870$ kg/m^3. The slider has a total mass equal to half the mass of the coupler $m_{\rm sl} = 0.033$ kg. A simply supported condition is supposed for the coupler deformation field. This choice is motivated by the fact that the slider has a large inertia and does not allow elastic displacement at the tip.

An illustration of the system and the block diagram used to construct the model are provided is Fig. 7. To construct the crank slider a transfomer interconnection is first used to connect the slider to the flexible coupler. The motion of the slider is then computed in the coupler reference frame. Then the sliding constraint, that requires the vertical velocity of the slider to be null in the inertial frame, is imposed as follows

$$0 = \sin(\theta_{P_1}) v_{P_2}^x + \cos(\theta_{P_1}) v_{P_2}^y = \mathbf{R}_y(\theta_{P_1}) \mathbf{v}_{P_2},$$

where $\mathbf{R}_y$ is the second line of the rotation matrix and $\dot{\theta}_{P_1} = \omega_{P_1}^z$ is the angle defining the orientation of the coupler. The rigid crank velocity at the endpoint

$$\mathbf{v}_{\rm cr}(t) = -\omega_{\rm cr} L_{\rm cr} \sin(\omega_{\rm cr} t) \widehat{\mathbf{X}} + \omega_{\rm cr} L_{\rm cr} \cos(\omega_{\rm cr} t) \widehat{\mathbf{Y}}$$

has to be written in the coupler reference frame to get the input

$$\mathbf{u}_{\rm cl} = R(\theta_{P_1})^\top \mathbf{v}_{\rm cr}. \tag{48}$$

The resulting system is a quasi linear index-2 DAE of the form

$$\begin{bmatrix} \mathbf{M} & 0 & 0 \\ 0 & 0 & 0 \\ 0 & 0 & 0 \end{bmatrix} \begin{bmatrix} \dot{\mathbf{e}} \\ \dot{\boldsymbol{\lambda}}_0 \\ \dot{\boldsymbol{\lambda}}_u \end{bmatrix} = \begin{bmatrix} \mathbf{J}(\mathbf{e}) & \mathbf{G}_0^\top(\theta_{P_1}) & \mathbf{G}_u^\top \\ -\mathbf{G}_0(\theta_{P_1}) & 0 & 0 \\ -\mathbf{G}_u & 0 & 0 \end{bmatrix} \begin{bmatrix} \mathbf{e} \\ \boldsymbol{\lambda}_0 \\ \boldsymbol{\lambda}_u \end{bmatrix} + \begin{bmatrix} 0 \\ 0 \\ R(\theta_{P_1})^\top \end{bmatrix} \mathbf{v}_{\rm cr}$$

Setting the initial conditions properly is of utmost importance for a DAE solver. For this problem the beam is supposed undeformed at the initial time. The initial conditions for the rigid movement are then found using basic kinematics considerations. The system is then solved using the IDA algorithm available in the Assimulo library [2]. In Fig. 8 the midpoint deformation displacement $u_f^x(L_{\rm cl/2})$, $u_f^y(L_{\rm cl/2})$, normalized with respect to the coupler length, is reported. The resulting vertical displacement is in accordance with the results presented in [15]. The horizontal displacement exhibits high oscillations because of the higher eigenfrequencies of the longitudinal movement. This is due to the fact that null initial conditions are imposed on the deformation [33]. In order to obtain a smoother solution, the initial deformation has to be computed from the rigid initial condition.

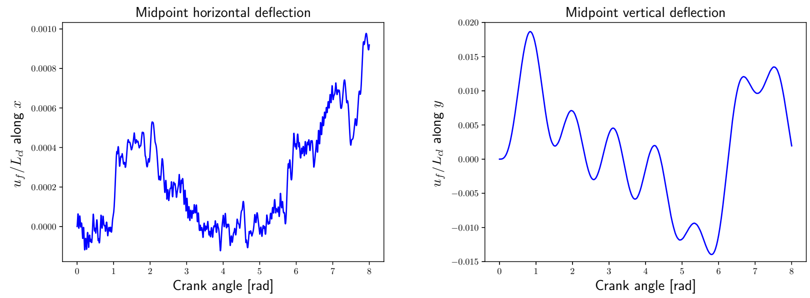

Fig. 8 Coupler midpoint horizontal (left) and vertical (right) displacement

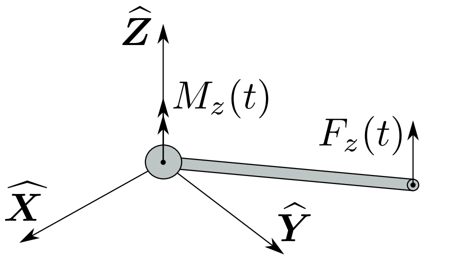

Fig. 9 Spatial beam on a spherical joint.

Table 2 Physical parameters for the hinged spatial beam.

Length	Cross section	Inertia moment	Density	Young modulus
141.45 [mm]	9.0 [mm^2]	6.75 [mm^4]	7800 [kg/mm^3]	2.1 10^6 [N/m^2]

6.3 Hinged spatial beam

A spatial beam rotating about a spherical joint is considered (see Fig. 9). This example was considered in [8,15]. The physical parameters are briefly recalled in Table 2. The spherical joint constraint is imposed by setting to zero the linear velocity, while a cantilever is imposed for the deformation field as the tip is free. For the first 10.2[s] a torque $M_z = 200$[N/mm] is applied about the vertical axis. Then, an impulsive force $F_z = 100$[N] is applied on tip of the beam at 15[s], to excite the out-of-plane movement. The system is solved using an implicit Runge-Kutta method of the Radau IIA family. The simulation results, provided in Fig. 10, corresponds to the kinetic energy and the angular velocity measured in the inertial vertical direction. The result matches with the provided references. Indeed the non linearities associated to the gyroscopic terms are small as the maximum angular velocity is equal to 0.1 rad/s $\approx$ 5 deg/s.

7 Conclusion

A port-Hamiltonian formulation for the flexible multibody dynamics has been discussed. The proposed methodology, being based on a floating frame formulation,

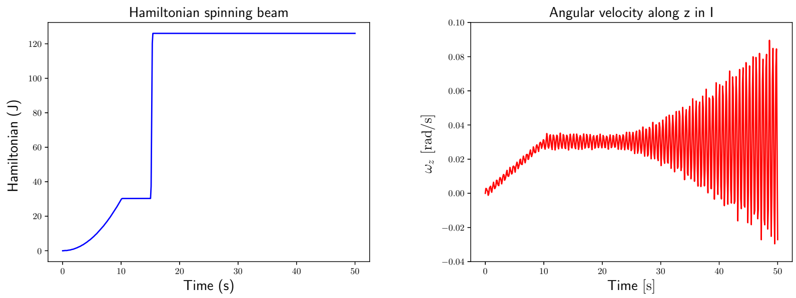

Fig. 10 Simulation results: kinetic energy (left) and angular velocity about the vertical inertial direction (right).

relies on the hypothesis of small deformations. However, the geometric stiffening effect can be accounted for by considering a corresponding energy. The discretization procedure uses a mixed finite element method, hence, the stress distribution is available without any post-processing. This is a valuable characteristic of this framework, as the stress distribution is the most important variable for preliminary analysis of mechanical components. Moreover, this approach allows to treat models easily (e.g. plates, shells). The construction of complex multibody system under this framework becomes completely modular and well suited for control application.
Many future directions are to be investigated. Large deformation could be included by employing a substructuring technique [32]. The stability and numerical convergence of the associated finite element is still to be proved. Another interesting topic is the application of model reduction techniques. While for linear pHDAE systems consolidated methodologies exist, for the general non linear differential-algebraic case, solutions are not yet available. The incorporation of control strategies is an important topic to be explored in the future.

Appendix A: Mathematical tools

We recall here some identities and definitions that will be used throughout the paper.

Properties of the cross product

We denote by $[\boldsymbol{a}]_\times$ the skew symmetric map associated to vector $\boldsymbol{a} = [a_x, a_y, a_z]^\top$

$$[\boldsymbol{a}]_\times = \begin{bmatrix} 0 & -a_z & a_y \\ a_z & 0 & -a_x \\ -a_y & a_x & 0 \end{bmatrix} \tag{49}$$

This map allows rewriting the cross product as a matrix vector product $\boldsymbol{a} \wedge \boldsymbol{b} = [\boldsymbol{a}]_\times \boldsymbol{b}$. The cross product satisfies the anticommutativity property

$$[\boldsymbol{a}]_\times \boldsymbol{b} = -[\boldsymbol{b}]_\times \boldsymbol{a}, \qquad \boldsymbol{a}, \boldsymbol{b} \in \mathbb{R}^3. \tag{50}$$

Furthermore, it satisfies the Jacobi Identity

$$[\boldsymbol{a}]_\times([\boldsymbol{b}]_\times\boldsymbol{c}) + [\boldsymbol{b}]_\times([\boldsymbol{c}]_\times\boldsymbol{a}) + [\boldsymbol{c}]_\times([\boldsymbol{a}]_\times\boldsymbol{b}) = 0, \qquad \boldsymbol{a},\boldsymbol{b},\boldsymbol{c} \in \mathbb{R}^3. \tag{51}$$

Adjointness of operators

In this paper, the adjoint of an operator is used. We recall the necessary definitions.

Definition 1 Given a linear operator $\mathcal{A} : \mathscr{H}^1 \to \mathscr{H}^2$ between Hilbert spaces the adjoint $\mathcal{A}^* : \mathscr{H}^2 \to \mathscr{H}^1$ fulfills

$$\langle y, \mathcal{A}x\rangle_{\mathscr{H}^2} = \langle \mathcal{A}^* y, x\rangle_{\mathscr{H}^1}, \qquad x \in \mathscr{H}^1, y \in \mathscr{H}^2. \tag{52}$$

To illustrate this definition, consider the operator $\mathcal{I}^\Omega = \int_\Omega(\cdot)\ \mathrm{d}\Omega : \mathscr{L}^2(\Omega,\mathbb{R}^3) \to \mathbb{R}^3$. Given a function $\boldsymbol{u} \in \mathscr{L}^2(\Omega,\mathbb{R}^3)$ and a vector $\boldsymbol{v} \in \mathbb{R}^3$, then the adjoint operator $(\mathcal{I}^\Omega)^*$ extends the vector $\boldsymbol{v}$ as a constant vector field over Ω

$$\langle \boldsymbol{v}, \mathcal{I}^\Omega \boldsymbol{u}\rangle_{\mathbb{R}^3} = \langle (\mathcal{I}^\Omega)^* \boldsymbol{v}, \boldsymbol{u}\rangle_{\mathscr{L}^2(\Omega,\mathbb{R}^3)}.$$

Definition 2 A bounded operator $\mathcal{A} : \mathscr{H} \to \mathscr{H}$ is self-adjoint if it holds

$$\langle y, \mathcal{A}x\rangle = \langle \mathcal{A}y, x\rangle, \qquad x, y \in \mathscr{H} \tag{53}$$

Definition 3 A bounded operator $\mathcal{A} : \mathscr{H} \to \mathscr{H}$ is skew-adjoint if it holds

$$\langle y, \mathcal{A}x\rangle = -\langle \mathcal{A}y, x\rangle, \qquad x, y \in \mathscr{H} \tag{54}$$

Indeed, the differential operators that appears in $\boldsymbol{\mathcal{J}}$ (Div, Grad), are unbounded in the L^2 topology. Whenever unbounded operators are considered, it is important to define their domain. To avoid the need of specifying domains, the notion of formal (or essential) adjoint can be evoked. The formal adjoint respects the integration by parts formula and is defined only for sufficiently smooth functions with compact support. In this sense Div, Grad are formally skew-adjoint, since for smooth functions with compact support, it holds

$$\langle y,\, \mathrm{Grad}(x)\rangle_{\mathscr{L}^2(\Omega,\mathbb{R}^{3\times 3}_{\mathrm{sym}})} \underbrace{=}_{\text{I.B.P.}} -\langle \mathrm{Div}(y),\, x\rangle_{\mathscr{L}^2(\Omega,\mathbb{R}^3)},$$

The definition of the domain of the operators, that requires the knowledge of the boundary conditions, has not been specified. For this reason, the $\boldsymbol{\mathcal{J}}$ operator is said to be formally skew-adjoint (or simply skew-symmetric).

Index of a differential-algebraic system

When dealing with differential-algebraic systems an important notion is the index.

Definition 4 The index of a DAE is the minimum number of differentiation steps required to transform a DAE into an ODE.

Because of their structure, pH multibody systems are of index two. Consider for simplicity a generic linear pH multibody system, whose equations are

$$\begin{aligned} \mathbf{M}\dot{\mathbf{e}} &= \mathbf{J}\mathbf{e} + \mathbf{G}^\top \boldsymbol{\lambda} + \mathbf{B}\mathbf{u}, \\ 0 &= -\mathbf{G}\mathbf{e}. \end{aligned}$$

Matrix $\mathbf{M}$ is squared and invertible and matrix $\mathbf{G}$ is full rank. If the second equation is derived twice in time, then it is obtained

$$\dot{\boldsymbol{\lambda}} = -(\mathbf{G}\mathbf{M}^{-1}\mathbf{G}^\top)^{-1}\mathbf{G}\mathbf{M}^{-1}(\mathbf{J}\dot{\mathbf{e}} + \mathbf{B}\dot{\mathbf{u}}).$$

Therefore, the system index is two.

Appendix B: Detailed derivation of the equation of motions

The detailed derivation of the pH system (12) is here presented. We stick to the notation adopted along the paper. First, let us recall the equations for a floating flexible body reported in [33,34].

– Linear momentum balance:

$$\begin{aligned} m {}^i\ddot{\boldsymbol{r}}_P + \boldsymbol{R}[\boldsymbol{s}_u]_\times^\top \dot{\boldsymbol{\omega}}_P + \boldsymbol{R}\int_\Omega \rho \ddot{\boldsymbol{u}}_f \,\mathrm{d}\Omega = \\ + \boldsymbol{R}\left\{ -[\boldsymbol{\omega}_P]_\times [\boldsymbol{\omega}_P]_\times \boldsymbol{s}_u - \int_\Omega 2\rho [\boldsymbol{\omega}_P]_\times \dot{\boldsymbol{u}}_f \,\mathrm{d}\Omega + \int_\Omega \boldsymbol{\beta} \,\mathrm{d}\Omega + \int_{\partial\Omega} \boldsymbol{\tau} \,\mathrm{d}\Gamma \right\} \end{aligned} \tag{55}$$

– Angular momentum balance:

$$\begin{aligned} [\boldsymbol{s}_u]_\times \boldsymbol{R}^\top {}^i\ddot{\boldsymbol{r}}_P + \boldsymbol{J}_u \dot{\boldsymbol{\omega}}_P + \int_\Omega \rho [\boldsymbol{x} + \boldsymbol{u}_f]_\times \ddot{\boldsymbol{u}}_f \,\mathrm{d}\Omega + [\boldsymbol{\omega}_P]_\times \boldsymbol{J}_u \boldsymbol{\omega}_P = \\ - \int_\Omega 2\rho [\boldsymbol{x} + \boldsymbol{u}_f]_\times [\boldsymbol{\omega}_P]_\times \dot{\boldsymbol{u}}_f \,\mathrm{d}\Omega + \int_\Omega [\boldsymbol{x} + \boldsymbol{u}_f]_\times \boldsymbol{\beta} \,\mathrm{d}\Omega + \int_{\partial\Omega} [\boldsymbol{x} + \boldsymbol{u}_f]_\times \boldsymbol{\tau} \,\mathrm{d}\Gamma \end{aligned} \tag{56}$$

– Flexibility PDE:

$$\rho \boldsymbol{R}^\top {}^i\ddot{\boldsymbol{r}}_P + \rho([\dot{\boldsymbol{\omega}}_P]_\times + [\boldsymbol{\omega}_P]_\times [\boldsymbol{\omega}_P]_\times)(\boldsymbol{x} + \boldsymbol{u}_f) + \rho(2[\boldsymbol{\omega}_P]_\times \dot{\boldsymbol{u}}_f + \ddot{\boldsymbol{u}}_f) = \mathrm{Div}\, \boldsymbol{\Sigma} + \boldsymbol{\beta}, \tag{57}$$

The first two equations are written in the inertial frame and so they need to be projected in the body frame. Considering that the position of point P, i.e. ${}^i\boldsymbol{r}_P$, is computed in the inertial frame and $\boldsymbol{v}_P$ in the body frame, it holds ${}^i\dot{\boldsymbol{r}}_P = \boldsymbol{R}\boldsymbol{v}_P$. The derivative of this gives

$$ {}^i\ddot{\boldsymbol{r}}_P = \boldsymbol{R}\left(\dot{\boldsymbol{v}}_P + [\boldsymbol{\omega}_P]_\times \boldsymbol{v}_P\right) \tag{58}$$

If (58) is put into (55), (56), (57) and pre-multiplying Eq. (55) by $\boldsymbol{R}^\top$, Eqs. (1) (2), (3) are obtained.

– Linear momentum balance:

$$\begin{aligned} &m(\dot{\boldsymbol{v}}_P + [\boldsymbol{\omega}_P]_\times \boldsymbol{v}_P) + [\boldsymbol{s}_u]_\times^\top \dot{\boldsymbol{\omega}}_P + \int_\Omega \rho \dot{\boldsymbol{v}}_f \,\mathrm{d}\Omega = \\ &\quad - [\boldsymbol{\omega}_P]_\times [\boldsymbol{\omega}_P]_\times \boldsymbol{s}_u - \int_\Omega 2\rho [\boldsymbol{\omega}_P]_\times \boldsymbol{v}_f \,\mathrm{d}\Omega + \int_\Omega \boldsymbol{\beta}\,\mathrm{d}\Omega + \int_{\partial\Omega} \boldsymbol{\tau}\,\mathrm{d}\Gamma. \end{aligned} \tag{59}$$

– Angular momentum balance:

$$\begin{aligned} &[\boldsymbol{s}_u]_\times(\dot{\boldsymbol{v}}_P + [\boldsymbol{\omega}_P]_\times \boldsymbol{v}_P) + \boldsymbol{J}_u \dot{\boldsymbol{\omega}}_P + \int_\Omega \rho [\boldsymbol{x}+\boldsymbol{u}_f]_\times \dot{\boldsymbol{v}}_f \,\mathrm{d}\Omega + [\boldsymbol{\omega}_P]_\times \boldsymbol{J}_u \boldsymbol{\omega}_P = \\ &- \int_\Omega 2\rho [\boldsymbol{x}+\boldsymbol{u}_f]_\times [\boldsymbol{\omega}_P]_\times \boldsymbol{v}_f \,\mathrm{d}\Omega + \int_\Omega [\boldsymbol{x}+\boldsymbol{u}_f]_\times \boldsymbol{\beta}\,\mathrm{d}\Omega + \int_{\partial\Omega} [\boldsymbol{x}+\boldsymbol{u}_f]_\times \boldsymbol{\tau}\,\mathrm{d}\Gamma. \end{aligned} \tag{60}$$

– Flexibility PDE:

$$\begin{aligned} \rho(\dot{\boldsymbol{v}}_P + [\boldsymbol{\omega}_P]_\times \boldsymbol{v}_P) + \rho([\dot{\boldsymbol{\omega}}_P]_\times + [\boldsymbol{\omega}_P]_\times [\boldsymbol{\omega}_P]_\times)(\boldsymbol{x}+\boldsymbol{u}_f) + \rho(2[\boldsymbol{\omega}_P]_\times \boldsymbol{v}_f + \dot{\boldsymbol{v}}_f) = \\ \mathrm{Div}\,\boldsymbol{\Sigma} + \boldsymbol{\beta}, \end{aligned} \tag{61}$$

where $\boldsymbol{v}_f = \dot{\boldsymbol{u}}_f$.

Consider now the term $[\boldsymbol{\omega}_P]_\times([\boldsymbol{\omega}_P]_\times \boldsymbol{s}_u)$, appearing in (59). Using the anticommutativity (50) and the fact that the cross map is skew-symmetric $[\boldsymbol{a}]_\times = -[\boldsymbol{a}]_\times^\top$ one finds

$$-[\boldsymbol{\omega}_P]_\times([\boldsymbol{\omega}_P]_\times \boldsymbol{s}_u) = [[\boldsymbol{s}_u]_\times^\top \boldsymbol{\omega}_P]_\times \boldsymbol{\omega}_P.$$

Eq. (59) is then rewritten as

$$\begin{aligned} &m\dot{\boldsymbol{v}}_P + [\boldsymbol{s}_u]_\times^\top \dot{\boldsymbol{\omega}}_P + \int_\Omega \rho \dot{\boldsymbol{v}}_f \,\mathrm{d}\Omega = \\ &\left[m\boldsymbol{v}_P + [\boldsymbol{s}_u]_\times^\top \boldsymbol{\omega}_P + 2\int_\Omega \rho \boldsymbol{v}_f \,\mathrm{d}\Omega\right]_\times \boldsymbol{\omega}_P + \int_\Omega \boldsymbol{\beta}\,\mathrm{d}\Omega + \int_{\partial\Omega} \boldsymbol{\tau}\,\mathrm{d}\Gamma. \end{aligned} \tag{62}$$

The terms $[\boldsymbol{s}_u]_\times([\boldsymbol{\omega}_P]_\times \boldsymbol{v}_P)$, $2\rho[\boldsymbol{x}+\boldsymbol{u}_f]_\times([\boldsymbol{\omega}_P]_\times \boldsymbol{v}_f)$, appearing in (60) can be rewritten using the Jacobi identity (51)

$$[\boldsymbol{s}_u]_\times([\boldsymbol{\omega}_P]_\times \boldsymbol{v}_P) = -[[\boldsymbol{s}_u]_\times \boldsymbol{v}_P]_\times \boldsymbol{\omega}_P - [[\boldsymbol{s}_u]_\times^\top \boldsymbol{\omega}_P]_\times \boldsymbol{v}_P, \tag{63}$$

$$2\rho[\boldsymbol{x}+\boldsymbol{u}_f]_\times([\boldsymbol{\omega}_P]_\times \boldsymbol{v}_f) = -[2\rho[\boldsymbol{x}+\boldsymbol{u}_f]_\times \boldsymbol{v}_f]_\times \boldsymbol{\omega}_P - [2\rho[\boldsymbol{x}+\boldsymbol{u}_f]_\times^\top \boldsymbol{\omega}_P]_\times \boldsymbol{v}_f \tag{64}$$

Eq. (60) is then rewritten as

$$
\begin{aligned}
&[\boldsymbol{s}_u]_\times \dot{\boldsymbol{v}}_P + \boldsymbol{J}_u \dot{\boldsymbol{\omega}}_P + \int_\Omega \rho [\boldsymbol{x} + \boldsymbol{u}_f]_\times \dot{\boldsymbol{v}}_f \, \mathrm{d}\Omega = \\
&\left[[\boldsymbol{s}_u]_\times^\top \boldsymbol{\omega}_P + 2 \int_\Omega \rho \boldsymbol{v}_f \, \mathrm{d}\Omega \right]_\times \boldsymbol{v}_P + \left[[\boldsymbol{s}_u]_\times \boldsymbol{v}_P + \boldsymbol{J}_u \boldsymbol{\omega}_P + 2 \int_\Omega \rho [\boldsymbol{x} + \boldsymbol{u}_f]_\times \boldsymbol{v}_f \, \mathrm{d}\Omega \right]_\times \boldsymbol{\omega}_P + \\
&2 \int_\Omega \left[\rho \boldsymbol{v}_P + \rho [\boldsymbol{x} + \boldsymbol{u}_f]_\times^\top \boldsymbol{\omega}_P \right]_\times \boldsymbol{v}_f \, \mathrm{d}\Omega + \int_\Omega [\boldsymbol{x} + \boldsymbol{u}_f]_\times \boldsymbol{\beta} \, \mathrm{d}\Omega + \int_{\partial\Omega} [\boldsymbol{x} + \boldsymbol{u}_f]_\times \boldsymbol{\tau} \, \mathrm{d}\Gamma.
\end{aligned} \tag{65}
$$

Notice that $2[\boldsymbol{v}_f]_\times \boldsymbol{v}_P + 2[\boldsymbol{v}_P]_\times \boldsymbol{v}_f = 0$. Using again the anticommutativity Eq. (61) is expressed as

$$
\begin{aligned}
&\rho \dot{\boldsymbol{v}}_P + \rho [\boldsymbol{x} + \boldsymbol{u}_f]_\times^\top \dot{\boldsymbol{\omega}}_P + \rho \dot{\boldsymbol{v}}_f = \\
&\left[\rho \boldsymbol{v}_P + \rho [\boldsymbol{x} + \boldsymbol{u}_f]_\times^\top \boldsymbol{\omega}_P + 2\rho \boldsymbol{v}_f \right]_\times \boldsymbol{\omega}_P + \mathrm{Div}\, \boldsymbol{\Sigma} + \boldsymbol{\beta}.
\end{aligned} \tag{66}
$$

Eqs. (62), (65), (66) are exactly (5), (6), (7). Now by definitions (13), (14)

$$
\begin{aligned}
\widetilde{\boldsymbol{p}}_t &= m \boldsymbol{v}_P + [\boldsymbol{s}_u]_\times^\top \boldsymbol{\omega}_P + 2 \int_\Omega \rho \boldsymbol{v}_f \, \mathrm{d}\Omega, \\
\widetilde{\boldsymbol{p}}_r &= [\boldsymbol{s}_u]_\times \boldsymbol{v}_P + \boldsymbol{J}_u \boldsymbol{\omega}_P + 2 \int_\Omega \rho [\boldsymbol{x} + \boldsymbol{u}_f]_\times \boldsymbol{v}_f \, \mathrm{d}\Omega, \\
\boldsymbol{\mathcal{I}}_{p_f}^\Omega(\cdot) &= \int_\Omega \left[2 \left(\rho \boldsymbol{v}_P + \rho [\boldsymbol{x} + \boldsymbol{u}_f]_\times^\top \boldsymbol{\omega}_P + \rho \boldsymbol{v}_f \right) + \rho \boldsymbol{v}_f \right]_\times (\cdot) \, \mathrm{d}\Omega,
\end{aligned}
$$

Eqs. (55), (56), (57) are written as

$$
\boldsymbol{\mathcal{M}} \frac{d}{dt} \begin{bmatrix} \boldsymbol{v}_P \\ \boldsymbol{\omega}_P \\ \boldsymbol{v}_f \\ \boldsymbol{\Sigma} \end{bmatrix} = \begin{bmatrix} 0 & [\widetilde{\boldsymbol{p}}_t]_\times & 0 & 0 \\ [\widetilde{\boldsymbol{p}}_t]_\times & [\widetilde{\boldsymbol{p}}_r]_\times & \boldsymbol{\mathcal{I}}_{p_f}^\Omega & 0 \\ 0 & -(\boldsymbol{\mathcal{I}}_{p_f}^\Omega)^* & 0 & \mathrm{Div} \\ 0 & 0 & \mathrm{Grad} & 0 \end{bmatrix} \begin{bmatrix} \boldsymbol{v}_P \\ \boldsymbol{\omega}_P \\ \boldsymbol{v}_f \\ \boldsymbol{\Sigma} \end{bmatrix} - \begin{bmatrix} 0 \\ 0 \\ \delta_{\boldsymbol{u}_f} H \\ 0 \end{bmatrix}, \tag{67}
$$

with

$$
\begin{aligned}
\boldsymbol{\mathcal{M}} &= \begin{bmatrix} m\boldsymbol{I}_{3\times 3} & [\boldsymbol{s}_u]_\times^\top & \mathcal{I}_\rho^\Omega & 0 \\ [\boldsymbol{s}_u]_\times & \boldsymbol{J}_u & \boldsymbol{\mathcal{I}}_{\rho x}^\Omega & 0 \\ (\mathcal{I}_\rho^\Omega)^* & (\boldsymbol{\mathcal{I}}_{\rho x}^\Omega)^* & \rho & 0 \\ 0 & 0 & 0 & \boldsymbol{\mathcal{D}}^{-1} \end{bmatrix}, \qquad \text{see (10)} \\
H &= \frac{1}{2} \int_\Omega \left\{ \rho ||\boldsymbol{v}_P + [\boldsymbol{\omega}_P]_\times (\boldsymbol{x} + \boldsymbol{u}_f) + \boldsymbol{v}_f||^2 + \boldsymbol{\Sigma} : \boldsymbol{\varepsilon} \right\} \mathrm{d}\Omega, \qquad \text{see (8)}.
\end{aligned}
$$

Hence, it is clear that Eqs. (55), (56), (57) from [33,34] are equivalently recast in form (12).

References

1. Alazard, D., Perez, J.A., Cumer, C., Loquen, T.: Two-input two-output port model for mechanical systems. DOI 10.2514/6.2015-1778. URL https://arc.aiaa.org/doi/abs/10.2514/6.2015-1778
2. Andersson, C., Führer, C., Åkesson, J.: Assimulo: A unified framework for {ODE} solvers. Mathematics and Computers in Simulation **116**(0), 26 – 43 (2015). DOI http://dx.doi.org/10.1016/j.matcom.2015.04.007
3. Arnold, D., Lee, J.: Mixed methods for elastodynamics with weak symmetry. SIAM Journal on Numerical Analysis **52**(6), 2743–2769 (2014). DOI 10.1137/13095032X
4. Beattie, C., Mehrmann, V., Xu, H., Zwart, H.: Linear port-Hamiltonian descriptor systems. Mathematics of Control, Signals, and Systems **30**(4), 17 (2018)
5. Brenan, K.E., Campbell, S.L., Petzold, L.R.: Numerical Solution of Initial-Value Problems in Differential-Algebraic Equations. Society for Industrial and Applied Mathematics (1995). DOI 10.1137/1.9781611971224. URL https://epubs.siam.org/doi/pdf/10.1137/1.9781611971224
6. Brugnoli, A., Alazard, D., Pommier-Budinger, V., Matignon, D.: Port-Hamiltonian formulation and symplectic discretization of plate models part I: Mindlin model for thick plates. Applied Mathematical Modelling **75**, 940 – 960 (2019). DOI 10.1016/j.apm.2019.04.035. URL https://doi.org/10.1016/j.apm.2019.04.035
7. Brugnoli, A., Alazard, D., Pommier-Budinger, V., Matignon, D.: Port-Hamiltonian formulation and symplectic discretization of plate models part II: Kirchhoff model for thin plates. Applied Mathematical Modelling **75**, 961 – 981 (2019). DOI 10.1016/j.apm.2019.04.036. URL https://doi.org/10.1016/j.apm.2019.04.036
8. Cardona, A.: Superelements modelling in flexible multibody dynamics. Multibody System Dynamics **4**(2), 245–266 (2000). DOI 10.1023/A:1009875930232. URL https://doi.org/10.1023/A:1009875930232
9. Cardoso-Ribeiro, F.L., Matignon, D., Lefèvre, L.: A partitioned finite element method for power-preserving discretization of open systems of conservation laws. arXiv preprint arXiv:1906.05965 (2019). Under review
10. Cervera, J., van der Schaft, A.J., Baños, A.: Interconnection of port-Hamiltonian systems and composition of dirac structures. Automatica **43**(2), 212–225 (2007). DOI 10.1016/j.automatica.2006.08.014
11. Chaturantabut, S., Beattie, C., Gugercin, S.: Structure-preserving model reduction for nonlinear port-Hamiltonian systems. SIAM Journal on Scientific Computing **38**(5), B837–B865 (2016). DOI 10.1137/15M1055085
12. Chebbi, J., Dubanchet, V., Perez Gonzalez, J.A., Alazard, D.: Linear dynamics of flexible multibody systems. Multibody System Dynamics **41**(1), 75–100 (2017). DOI 10.1007/s11044-016-9559-y. URL https://doi.org/10.1007/s11044-016-9559-y
13. Duindam, V., Macchelli, A., Stramigioli, S., Bruyninckx, H.: Modeling and Control of Complex Physical Systems. Springer Verlag (2009). URL https://www.springer.com/us/book/9783642031953
14. Egger, H., Kugler, T., Liljegren-Sailer, B., Marheineke, N., Mehrmann, V.: On structure-preserving model reduction for damped wave propagation in transport networks. SIAM Journal on Scientific Computing **40**(1), A331–A365 (2018). DOI 10.1137/17M1125303
15. Ellenbroek, M., Schilder, J.: On the use of absolute interface coordinates in the floating frame of reference formulation for flexible multibody dynamics. Multibody System Dynamics **43**(3), 193–208 (2018). DOI 10.1007/s11044-017-9606-3. URL https://doi.org/10.1007/s11044-017-9606-3
16. Forni, P., Jeltsema, D., Lopes, G.A.: Port-Hamiltonian formulation of rigid-body attitude control. IFAC-PapersOnLine **48**(13), 164 – 169 (2015). DOI https://doi.org/10.1016/j.ifacol.2015.10.233. URL http://www.sciencedirect.com/science/article/pii/S2405896315021242. 5th IFAC Workshop on Lagrangian and Hamiltonian Methods for Nonlinear Control LHMNC 2015
17. Golo, G., Talasila, V., van der Schaft, A.J., Maschke, B.: Hamiltonian discretization of boundary control systems. Automatica **40**(5), 757–771 (2004). DOI 10.1016/j.automatica.2003.12.017. URL http://dx.doi.org/10.1016/j.automatica.2003.12.017
18. Hurty, W.C.: Dynamic analysis of structural systems using component modes. AIAA Journal **3**(4), 678–685 (1965). DOI 10.2514/3.2947. URL https://doi.org/10.2514/3.2947

19. Kitis, L., Lindenberg, R.: Natural frequencies and mode shapes of flexible mechanisms by a transfer matrix method. Finite Elements in Analysis and Design **6**(4), 267 – 285 (1990). DOI 10.1016/0168-874X(90)90020-F. URL `https://doi.org/10.1016/0168-874X(90)90020-F`
20. Klerk, D.D., Rixen, D.J., Voormeeren, S.N.: General framework for dynamic substructuring: History, review and classification of techniques. AIAA Journal **46**(5), 1169–1181 (2008). DOI 10.2514/1.33274. URL `https://doi.org/10.2514/1.33274`
21. Leyendecker, S., Betsch, P., Steinmann, P.: The discrete null space method for the energy-consistent integration of constrained mechanical systems. part III: Flexible multibody dynamics. Multibody System Dynamics **19**(1), 45–72 (2008). DOI 10.1007/s11044-007-9056-4. URL `https://doi.org/10.1007/s11044-007-9056-4`
22. Macchelli, A., Melchiorri, C., Stramigioli, S.: Port-based modeling of a flexible link. IEEE Transactions on Robotics **23**, 650 – 660 (2007). DOI 10.1109/TRO.2007.898990
23. Macchelli, A., Melchiorri, C., Stramigioli, S.: Port-based modeling and simulation of mechanical systems with rigid and flexible links. IEEE Transactions on Robotics **25**(5), 1016–1029 (2009). DOI 10.1109/TRO.2009.2026504
24. Mehrmann, V., Morandin, R.: Structure-preserving discretization for port-Hamiltonian descriptor systems. In: Proceedings of the 59th IEEE Conference on Decision and Control, pp. 6663 – 6868 (2019)
25. Nageshrao, S.P., Lopes, G.A.D., Jeltsema, D., Babuška, R.: Port-hamiltonian systems in adaptive and learning control: A survey. IEEE Transactions on Automatic Control **61**(5), 1223–1238 (2016). DOI 10.1109/TAC.2015.2458491
26. Nowakowski, C., Fehr, J., Fischer, M., Eberhard, P.: Model order reduction in elastic multibody systems using the floating frame of reference formulation. IFAC Proceedings Volumes **45**(2), 40 – 48 (2012). DOI https://doi.org/10.3182/20120215-3-AT-3016.00007. URL `http://www.sciencedirect.com/science/article/pii/S1474667016306401`. 7th Vienna International Conference on Mathematical Modelling
27. Ortega, R., García-Canseco, E.: Interconnection and damping assignment passivity-based control: A survey. European Journal of Control **10**(5), 432 – 450 (2004)
28. Perez, J.A., Alazard, D., Loquen, T., Pittet, C., Cumer, C.: Flexible Multibody System Linear Modeling for Control Using Component Modes Synthesis and Double-Port Approach. Journal of Dynamic Systems, Measurement, and Control **138**(12) (2016). DOI 10.1115/1.4034149. URL `https://doi.org/10.1115/1.4034149`. 121004
29. Rathgeber, F., Ham, D., Mitchell, L., Lange, M., Luporini, F., McRae, A.T., Bercea, G., Markall, G.R., Kelly, P.: Firedrake: automating the finite element method by composing abstractions. ACM Transactions on Mathematical Software (TOMS) **43**(3), 24 (2017)
30. Rui, X., He, B., Lu, Y., Lu, W., Wang, G.: Discrete time transfer matrix method for multibody system dynamics. Multibody System Dynamics **14**(3), 317–344 (2005). DOI 10.1007/s11044-005-5006-1. URL `https://doi.org/10.1007/s11044-005-5006-1`
31. Sanfedino, F., Alazard, D., Pommier-Budinger, V., Falcoz, A., Boquet, F.: Finite element based N-port model for preliminary design of multibody systems. Journal of Sound and Vibration **415**, 128 – 146 (2018). DOI https://doi.org/10.1016/j.jsv.2017.11.021. URL `http://www.sciencedirect.com/science/article/pii/S0022460X17307915`
32. Shabana, A.: Substructure synthesis methods for dynamic analysis of multi-body systems. Computers & Structures **20**(4), 737 – 744 (1985). DOI https://doi.org/10.1016/0045-7949(85)90035-5. URL `http://www.sciencedirect.com/science/article/pii/0045794985900355`
33. Simeon, B.: DAEs and PDEs in elastic multibody systems. Numerical Algorithms **19**(1), 235–246 (1998). DOI 10.1023/A:1019118809892. URL `https://doi.org/10.1023/A:1019118809892`
34. Simeon, B.: Computational flexible multibody dynamics. Springer (2013)
35. Steinbrecher, A.: Numerical solution of quasi-linear differential-algebraic equations and industrial simulation of multibody systems. Ph.D. thesis, TU Berlin (2006). DOI 10.14279/depositonce-1360
36. Tan, T., Yousuff, A., Bahar, L., Konstantinidis, M.: A modified finite element-transfer matrix for control design of space structures. Computers & Structures **36**(1), 47 – 55 (1990). DOI https://doi.org/10.1016/0045-7949(90)90173-Y. URL `http://www.sciencedirect.com/science/article/pii/004579499090173Y`
37. Wasfy, T.M., Noor, A.K.: Computational strategies for flexible multibody systems . Applied Mechanics Reviews **56**(6), 553–613 (2003). DOI 10.1115/1.1590354. URL `https://asmedigitalcollection.asme.org/appliedmechanicsreviews/article-pdf/56/6/553/5440485/553_1.pdf`

38. Young, K.D.: Distributed finite-element modeling and control approach for large flexible structures. Journal of Guidance, Control, and Dynamics **13**(4), 703–713 (1990). DOI 10.2514/3.25389. URL `https://doi.org/10.2514/3.25389`